Research Technical Completion Report

INTERACTION OF SYNTHETIC ORGANIC CONTAMINANTS WITH NATURAL COLLOIDAL MATERIALS

by

M.J. Morra

Department of Plant, Soil and Entomological Sciences

Idaho Water Resources Research Institute
University of Idaho
Moscow, Idaho 83843

September, 1990

The research on which this report is based was financed in part by the United States Department of the Interior as authorized by the Water Research and Development Act of 1978 (P.L. 95-467).

Research Technical Completion Report

14-08-0001-G1559-02

INTERACTION OF SYNTHETIC ORGANIC CONTAMINANTS WITH NATURAL COLLOIDAL MATERIALS

by

M.J. Morra

Department of Plant, Soil and Entomological Sciences

Submitted to

U.S. Geological Survey
U.S. Department of Interior
Washington, D.C. 20242

Idaho Water Resources Research Institute
University of Idaho
Moscow, Idaho 83843

September, 1990

TABLE OF CONTENTS

LIST OF FIGURES

LIST OF FIGURES (cont.)

LIST OF TABLES

ABSTRACT

Groundwater represents the source of 90% of Idaho's public water supply, thus making potential pesticide contamination a key issue. A small, but significant portion of the applied pesticide is transported through the soil column more quickly than predicted by currently available models. It has been proposed that increased pesticide mobility occurs as a result of pesticide complexation with colloidal soil constituents, such that the pesticide-colloid complex moves faster than the pesticide alone.

The objectives of the research in progress are to 1) develop the methodologies for qualitatively and quantitatively studying pesticide complexation with colloidal soil materials, 2) define the key variables controlling complexation, 3) compare predicted complexation and pesticide mobility alteration with actual results obtained in simulated field situations, and 4) propose a model input variable to produce more accurate estimates of pesticide transport in soil.

This report presents the second year results of the three-year study, focusing on objectives 1 and 2. It is organized in chapters, each of which is intended as a separate peer review publication. We have: obtained the spectra of humic materials in aqueous solution; developed methods to obtain unaltered organo-mineral colloids from soils and non-destructively measured the C and N content of these colloids; extensively studied the fluorescence characteristics of a cationic herbicide (difenzoquat); and confirmed that humic acid interacts with nonionic synthetic organic compounds in a partitioning manner and therefore is a potential carrier for nonionic contaminants in soil.

INTRODUCTION

Groundwater represents the source of 90% of Idaho's public water supply. Preservation of groundwater quality is therefore a high priority within the state, particularly in the northern Rathdrum Prairie area. The underlying aquifer was designated as one of three sole-source aquifers in the U.S. by the EPA. Groundwater contamination by DCPA and aldicarb has been detected in southwestern Idaho (Bruck, 1986) and by dinoseb, picloram, and dicamba in the Boise area (J. Baldwin, Dept. of Health and Welfare, Div. of the Environ., Boise, ID, personal communication). Regular monitoring of contaminant concentrations present in groundwater is not feasible because of the large number of different synthetic organics used and the lack of a sufficient quantity and distribution of monitoring wells. In addition, groundwater reclamation is costly, thus necessitating the recognition of potential contamination problems.

Currently available models do not accurately predict the transport of synthetic organic contaminants in the environment. It has recently been proposed that one of the reasons organic contaminants are transported more quickly than predicted is because of complexation with a water soluble soil organic fraction of unknown chemical structure (Bowman and Rice, 1986; Jury et al., 1986; Enfield and Bengtsson, 1986). Complexation may not only increase the water solubility of hydrophobic compounds (Chiou et al., 1986), but alter pesticide charge and size characteristics (Tramonti et al., 1986). Laboratory studies concerning the determination of synthetic organic compound partitioning between solid (soil) and liquid (water) phases have used complexation with a water soluble organic material as the reason for discrepancies between

actual and predicted partitioning (Gschwend and Wu, 1985; Voice et al., 1983; Voice and Weber, 1985). An interaction between synthetic organic compounds and soluble humic materials has been demonstrated (Madhun, et al., 1986; Ballard, 1971; Caron et al., 1985; Wijayaratne and Means, 1984; Sullivan and Felbeck, 1968; Senesi and Testini, 1982; Carter and Suffet, 1982), but the type of association is uncertain (Wijayaratne and Means, 1984; Chiou et al., 1983). Chiou and co-workers have suggested that hydrophobic organic compounds partition into the hydrophobic interior of humic materials (Chiou et al., 1986). Lee and Farmer (1989) also concluded that partitioning may occur, but suggest that polarity of the synthetic organic compound and specific characteristics of the organic matter must be considered.

A mathematical relationship between dissolved organic carbon (water soluble soil organic materials) and relatively immobile chemicals has been proposed for inclusion in pesticide transport models (Enfield, 1985; Enfield and Bengtsson, 1986). Computer simulation demonstrated that measurable increases in mobility of the chemicals may occur through an interaction with water soluble soil organic materials (Enfield, 1985). More recent work by Enfield and co-workers has shown faster movement of colloid complexes than the uncomplexed synthetic organic compounds in actual column experiments (Enfield et al., 1989).

Although the incorporation of this parameter into a model describing contaminant transport thus appears to be critical, the proponents acknowledge that the approach is currently limited by a lack of data describing the physical and chemical processes occurring during complexation and contaminant movement. In other words, contaminant complexation with a water soluble soil organic material can cause

increased mobility, but an inadequate understanding of the interaction itself prohibits the development of an accurate model input parameter.

Interaction of organic pollutants with inorganic clay colloids has also been suggested as a possible mechanism for facilitating contaminant movement (Jury and Ghodrati, 1987). Even less is known about the potential of clays to enhance organic contaminant mobility than for natural colloidal organic materials. Again, inclusion of a parameter describing these interactions into hydrologic models has not been achieved as a result of inadequate knowledge concerning fundamental interaction mechanisms and complex stability.

Recent reviews have clearly shown that inorganic and organic colloids exert a tremendous influence on synthetic organic compounds in both soil and subsurface environments (Huling, 1989; McCarthy and Zachara, 1989). However, a number of key questions remain unanswered.

The objectives of the research in progress are to 1) develop the methodologies for qualitatively and quantitatively studying pesticide complexation with colloidal soil materials, 2) define the key variables controlling complexation, 3) compare predicted complexation and pesticide mobility alteration with actual results obtained in simulated field situations, and 4) propose a model input variable to produce more accurate estimates of pesticide transport in soil.

This report presents the second year results of the three-year study, focusing on objectives 1 and 2. It is organized in chapters, each of which is intended as a separate peer review publication. We have: obtained the spectra of humic materials in aqueous solution (Appendix A); developed methods to obtain unaltered organo-mineral colloids from soils (p. 5) and non-destructively measured the C and N

content of these colloids (p. 29); extensively studied the fluorescence characteristics of a cationic herbicide (difenzoquat) (p. 42); and confirmed that humic acid interacts with nonionic synthetic organic compounds in a partitioning manner and therefore is a potential carrier for nonionic contaminants in soil (56).

This research has required collaboration with a number of individuals at both the University of Idaho as well as other institutions.

Dr. Robert R. Blank, USDA/ARS, 920 Valley Road Reno, NV 89512

Dr. Ray M.A. von Wandruszka, Dept. of Chemistry, Univ. of Idaho, Moscow, ID 83843

Dr. W.Daniel Edwards, Dept. of Chemistry, Univ. of Idaho, Moscow, ID 83843

Dr. Marvin H. Hall, Div. of Plant Science, Univ. of Idaho, Moscow, ID 83843

Dr. David B. Marshall, Dept. of Chemistry and Biochemistry, Utah State Univ., Logan, UT 84322

SIZE FRACTIONATION OF SOIL ORGANO-MINERAL COMPLEXES USING ULTRASONIC DISPERSION

Matthew J. Morra, Robert R. Blank, and Larry L. Freeborn

Abstract

Potential artifacts created by soil fractionation procedures are frequently ignored when studying the interaction of natural and synthetic organic compounds with clay-sized materials. Ultrasonic dispersion treatments of 0, 0.32, 0.84, 1.37, 2.94, 4.51, and 7.66 kJ were used in combination with centrifugation and sedimentation techniques to obtain sand (2.0-0.05 mm), silt (50-2 μm), coarse clay (2.0-0.02 μm), and medium clay (0.2-0.08 μm) fractions from soils with organic C contents of 19.2 to 44.2 g kg^{-1}. No more than 1.37 kJ of sonication energy was needed for maximum yields of silt-sized materials, whereas sand yields decreased logarithmically and clay yields increased quadratically with energy inputs up to 7.66 kJ. Coulter counter analysis of silt-sized fractions showed that no redistribution of particle-size occurred within this fraction with increased sonication energy. Total C and N concentrations in the silt-sized fraction were not consistently altered with increased sonication energy. Total C and N concentrations in the coarse clay- and medium clay-sized fractions increased and decreased, respectively, with increased sonication energy. Diffuse reflectance FT-IR analysis did not detect any changes in the coarse clay fractions, while changes in the medium clay fractions of the two soils highest in organic C occurred when energy was increased from 0.84 to 2.94 kJ. Maximizing soil dispersion by using excessive

sonication energies may create undesirable artifacts especially to the 0.2 to 0.08 μm clay-sized fraction. It is suggested that a standard sonication energy between 3 to 5 kJ and a soil to water ratio of 1 to 5 be used to obtain adequate particle size yields and limit artifacts in the fractionated organo-mineral complexes.

Introduction

Reactions of both recognizable biochemical compounds and humic substances with inorganic soil materials influence the chemical, physical, and biological properties of soils (Schnitzer, 1986; Hayes and Himes, 1986; Mortland, 1986). Conversely, the mobility and reactivity of natural organic compounds in soil are controlled by interactions with inorganic soil constituents. The adsorption and reactions of synthetic organic compounds with inorganic surfaces in soil is also important because of increased concern over environmental contamination by pesticides and industrial chemicals (Zielke et al., 1989). Recent reviews have shown that colloidal constituents may increase the mobility of synthetic organic compounds in both soil and subsurface environments by acting as vehicles of transport (Huling, 1989; McCarthy and Zachara, 1989). The potential reactions occurring between both natural and synthetic organic compounds and inorganic soil materials have been previously reviewed (Theng, 1974; Schnitzer and Khan, 1972; Theng, 1979).

Clay-sized materials are most important because of their large surface areas and high cation exchange capacities. An often used approach to study interactions of natural and synthetic organic compounds with discrete particle size fractions is to use commercially

available clay-sized materials. However, it is well established that most clays exist in soil as part of an organo-mineral complex (Hayes and Himes, 1986). The use of "clean" or commercially available clays therefore, fails to accurately simulate the actual soil system.

A more appropriate approach is to separate organo-mineral complexes from whole soils. This can be achieved by a variety of methods, but it is essential that harsh chemical pretreatments be avoided. The most obvious approach is to disperse the soil by shaking as a water slurry. However, extended shaking times can alter organo-mineral complexes through abrasion (Watson, 1971). In addition, interlaboratory transfer is not easily achieved because of an inability to directly quantify the energy input used for dispersion. An alternative approach is to use ultrasonic energy for soil dispersion followed by a series of sieving and sedimentation fractionation steps. Sonication allows the application of a readily measured and reproducible dispersion energy. The use of sonication for soil dispersion has been the subject of numerous investigations over the past twenty years (Chichester, 1969; Genrich and Bremner, 1972; Genrich and Bremner, 1974; Watson and Parsons, 1974; Hinds and Lowe, 1980; Anderson et al., 1981; Hunter and Busacca, 1989; Gregorich et al., 1989). Christensen (1985) has provided the most comprehensive summary of the wide variety of sonication energies used in previous studies. However, it is well appreciated that sonication energy may create artifacts or in some manner alter the resulting organo-mineral complexes (Watson, 1971; Bruckert, 1982; Spycher and Young, 1977).

Previous studies have not adequately determined the impact of increased sonication energy on the qualitative nature of the organo-

mineral complexes, but have focused mainly on particle size yields. Our objective is to develop a method to separate organo-mineral complexes from soil with as little alteration as possible. More specifically, our purpose is to determine the maximum input energy that can be used for this separation. Sonication was chosen as the dispersion method in order to facilitate standardization and thus interlaboratory transfer of this technique.

Materials and Methods

Soils

Four soils were selected to obtain a range in organic C and free carbonates (Table 1.1). Surface soil samples (0-15 cm) were collected, air-dried, and sieved (2 mm). Analyses were conducted using the following methods: pH by glass electrode (1:1 soil to water), organic C by the Walkley-Black method (Nelson and Sommers, 1982), and total C and N by Dumas combustion (LECO CHN-600 Determinator, St. Joseph, MI). Particle size distributions were determined using methods similar to those of Jackson (1956) and will be discussed in detail in the following section. Clay sized minerals were identified using x-ray diffraction (Table 1.2).

Chemical Dispersion

The method used to determine particle size distributions involved the removal of carbonates, organic matter, and exchangeable ions prior to dispersion with sodium hexametaphosphate (Jackson, 1956). This method, designated as PSD in the text, figures, and tables, was used as

Table 1.1. Characteristics of soils used in sonication experiments.

Soil			Total carbon	Organic carbon	Total nitrogen	Clay	Sand
Series	Subgroup	pH	g kg^{-1}				
Nyssaton sil	Xerollic Calciorthids	6.9	20.2	8.5	0.8	71	263
Palouse sil	Pachic Ultic Haploxerolls	5.7	19.5	19.2	1.6	211	88
Latahco sil	Argiaquic Xeric Argialbolls	6.1	41.0	41.0	3.9	159	122
Sudduth sil	Argic Pachic Cryoboralls	5.6	47.5	44.2	3.2	244	166

Table 1.2. Mineralogical characteristics of soils used in sonication experiments.

Soil	Mineralogy[a]
Nyssaton	smectite (hydroxy-interlayered), kaolinite (holloysite), mica
Palouse	mica, kaolinite, vermiculite
Latahco	mica, kaolinite, smectite
Sudduth	short-range ordered minerals (allophane, imogolite), kaolinite (holloysite)

[a]Mineral components arranged in descending order of proportion within each respective soil.

the reference method to compare with particle size distributions obtained using ultrasonic dispersion on otherwise untreated soils.

Carbonates were removed by addition of 1 M HCl (35 ml) to 12 g soil. Samples were centrifuged at 336 x g for 15 min and the clear liquid decanted. The remaining sample was washed with deionized water and centrifuged as above with the addition of 5 drops of NaCl in those instances in which centrifugation did not remove suspended clay-sized particles. Organic matter was digested by addition of 30% H_2O_2 and the soil sample was again separated from the supernatant using centrifugation (Day, 1965). Exchangeable cations were removed by washing twice with 95% methanol (adjusted to pH 3.0 with HCl) and once with 95 % ethanol (Jackson, 1956). Centrifugation was performed between all washes. The samples were dried at 105°C for 24 hours and the mass recorded. Dispersion was performed by the addition of 10 ml of 5% sodium hexametaphosphate followed by shaking for 16 h on a reciprocating shaker.

Sonication

Dispersion by sonication was performed by placing 10 g soil and 50 ml of water into a 100 ml plastic centrifuge tube, stirring with a glass rod, and applying 0.32, 0.84, 1.37, 2.94, 4.51, or 7.66 kJ of energy using a Biosonic III probe type sonifier (Bronwill Scientific, Rochester, NY). Time of energy application required to achieve the total input energies above ranged from 0 to 300 s. Maximum temperature increase of the soil-water mixture with an input energy of 7.66 kJ was 30°C.

Energy output from the probe tip and calibration with instrument intensity settings was performed according to North (1976). The

increase in temperature (ΔT) produced by sonicating a known mass of water (mw) in a Dewar flask for a specific time period (t) was measured using a precalibrated thermocouple connected to a data logger. Probe output energy (P) in J sec^{-1} was calculated by the equation:

$$P = (m_w c_w + w_r) \frac{\Delta T}{t} + H \qquad (1)$$

where c_w is the mean specific heat of water taken to be 4.180 J $(g\ K)^{-1}$, H is heat loss, and w_r the thermal capacity of the Dewar flask. H in J sec^{-1} was determined by measuring the rate of water cooling in an undisturbed Dewar flask. w_r was determined using the method of mixtures according to the following equation (Weast, 1975).

$$m_1 s\ (T_1 - T_3) = (m_3 c + m_2 c_w)\ (T_3 - T_2) \qquad (2)$$

s is the specific heat of the substance with mass of m_1 at a temperature of T_1. This substance is placed in a second mass, m_2, of water at temperature T_2, resulting in temperature T_3. m_3 and c are the mass and specific heat of the calorimeter, respectively. c_w is the specific heat of water, which in this case equals s. w_r in J K^{-1} is equal to $m_3 c$.

Probe calibration using equation (1) was conducted with emersion of the probe tip 1.5 cm below the water's surface and resulted in total output energies (E = P x t) linearly related to time of sonication according to the following equation.

$$E = 20.92\ J\ sec^{-1}\ (t) - 139.36\ J \qquad (3)$$

Emersion of the probe tip to a depth of 5.5 cm also resulted in a linear relationship.

$$E = 31.50 \text{ J sec}^{-1} (t) - 64.89 \text{ J} \quad (4)$$

Both calibration equations had r^2 values of 0.99.

Particle-size Separation

The suspension was washed through a 300 mesh sieve with 450 ml of water and the sand and large silt remaining on the sieve were rinsed with a small amount of acetone and dried at 105°C for 2 h. Silts were separated from the sand by sieving and the dry weight recorded. Centrifugal separations of the remaining size fractions were performed according to Stoke's Law (Jackson, 1956). Silt was separated from clay-sized material by centrifugation (IEC Model K, Needham Heights, MA) at 131 x g for 170 s at 26°C and freeze-dried. Coarse clay (2.0-0.2 μm) was separated from the suspension by centrifugation at 932 x g for 39.5 min at 26°C. Medium clay (0.2-0.08 μm) was separated from the remaining suspension by centrifugation at 12,969 x g for 9.4 min at 20°C using an IEC B20A refrigerated centrifuge (Needham Heights, MA). Both the coarse and medium size clay fractions were freeze-dried, weighed, lightly crushed with a mortar and pestle, and stored at room temperature.

Models of Particle-size Yields

Regression analysis was performed on yields of sand, silt, and clay obtained from each of the soils with different sonication energies (Steele and Torrie, 1960). Linear-plateau regression models (Anderson and Nelson, 1975) were applied according to the following equation:

$$y = b_0 + b_1 [\min(X,A)] \quad (5)$$

where b_0 is the intercept and b_1 is the slope of the line up to the point X = A. All of the data were first analyzed using linear

regression analysis. The largest value of X was then deleted and residuals obtained. The residuals about the higher values of X were computed and added to those computed initially. The point at which the combined residuals reached a minimum was selected as the plateau intersection, and thus the point at which X = A. A second model was used to determine if a significant slope (b_2) existed beyond the point of X = A.

$$y = b_0 + b_1[\min(X,A)] + b_2[\max(X,A) - A] \quad (6)$$

Silt and Clay Analysis

Size distribution of the silt-sized fraction was determined using a Coulter Counter model TAII (Hialeah, FL). A silt suspension was prepared by adding 0.5 g freeze-dried silt to 50 ml of 0.05% sodium hexametaphosphate solution. The suspension was shaken for 18 h and analyzed using a 140 μm aperature tube.

Total C and N in the silt, coarse clay, and medium clay were determined on duplicate samples by Dumas combustion (LECO CHN-600 Determinator, St. Joseph, MI).

Infrared analysis of the coarse and medium sized clay fractions was performed using a Digilab FTS-80 FT-IR spectrometer equipped with a MCT detector. A diffuse reflectance sample cell fitted with a macro sample cup (Collector^{TM}, Spectra·Tech, Stamford, CT) was used to obtain all spectra. Spectra were recorded in the absorbance mode from 670 to 4000 cm^{-1} and signal averaged for 256 scans. The spectra were obtained by referencing a background KBr spectrum to the sample spectrum.

Results and Discussion

Particle Size Yields

Particle size yields varied with the energy of sonication. Sand yields decreased rapidly with sonication energies up to 1.36 kJ (Fig. 1.1). Additional sonication energy from 1.36 to 7.66 kJ decreased yields, but at a rate that appears to be reaching an asymptotic limit. Clay yields showed the opposite trend, but start to reach a maximum at higher sonication energies of approximately 4.51 kJ (Fig. 1.2). Silt yields reached a maximum at lower sonication energies of 0.32 to 0.84 kJ (Fig. 1.3). Three distinctly different models were fit to the three particle size yields (Table 1.3). Linear plateau regression demonstrated that only the silt-size fraction reached a true maximum at the sonication energies used. The amount of soil organic matter and free carbonates does not appreciably alter the model relationships, in that particle-size yields from all soils responded similarly.

In most instances when sonication has been used as the technique for soil dispersion, one specific sonication time (energy) was chosen to maximize particle size yields (Chichester, 1969; Watson and Parsons, 1974; Genrich and Bremner, 1974; Hinds and Lowe, 1980a; Hinds and Lowe, 1980b; Ahmed and Oades, 1984; Anderson et al., 1981; Hamblin, 1977). Little consideration was given to possible artifacts created during the procedure. In addition, a large proportion of the research was conducted without proper calibration of the energy output from the sonicator probe (Hinds and Lowe, 1980a; Hinds and Lowe, 1980b; Ahmed and Oades, 1984; Anderson et al., 1981; Hamblin, 1977). Without such information it is impossible to reproduce those studies.

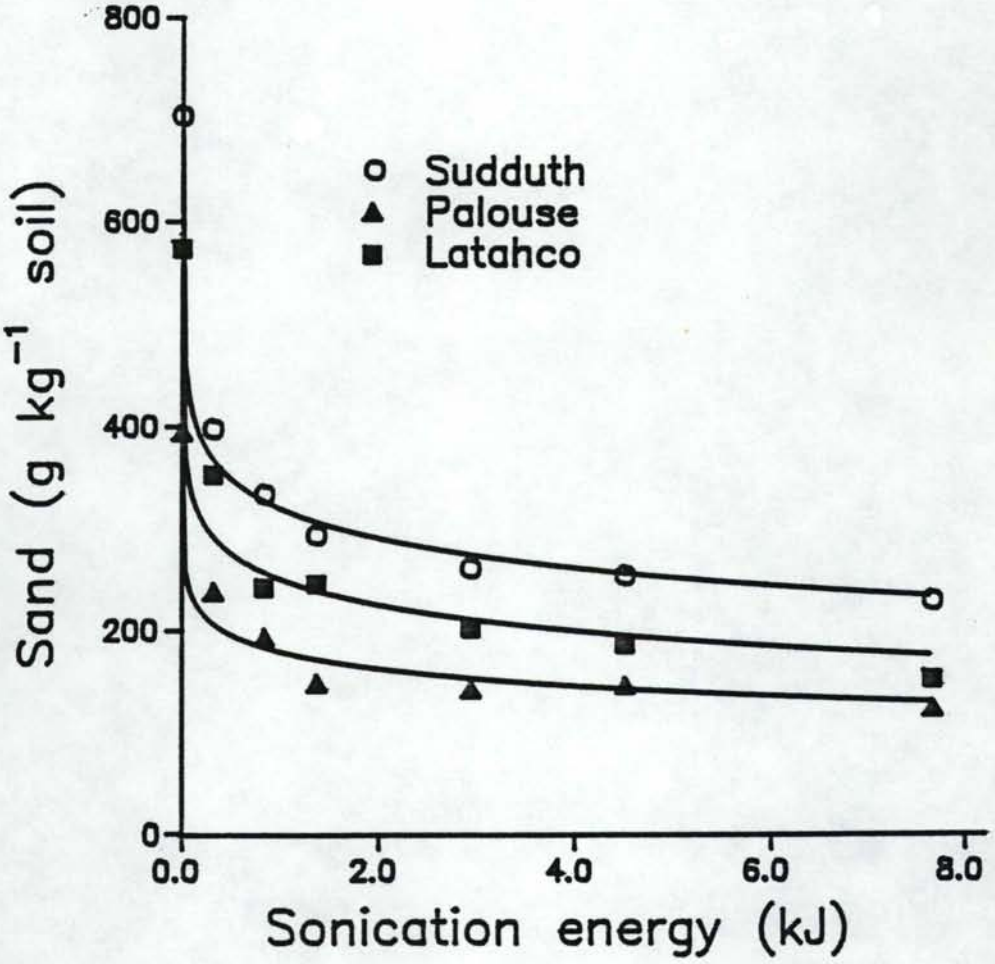

Fig. 1.1. Yields of sand-sized particles from soil after sonication at different energies.

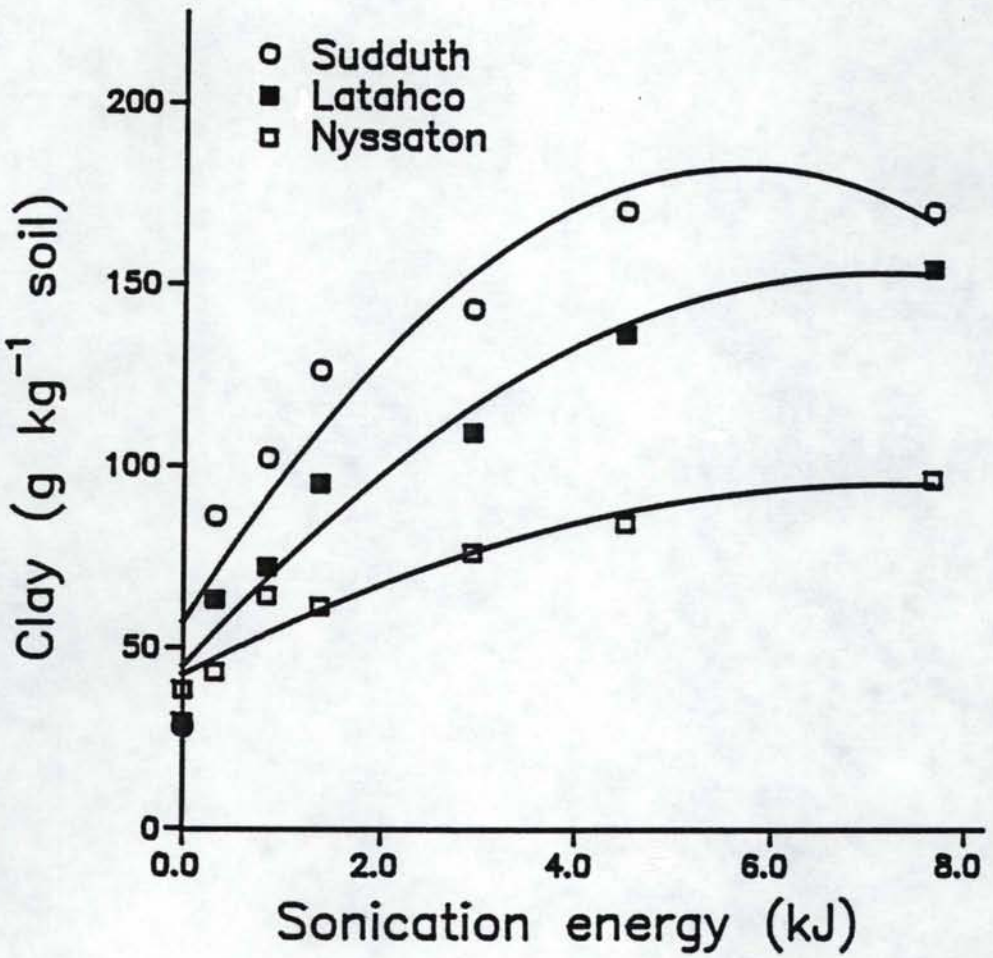

Fig. 1.2. Yields of clay-sized particles from soil after sonication at different energies.

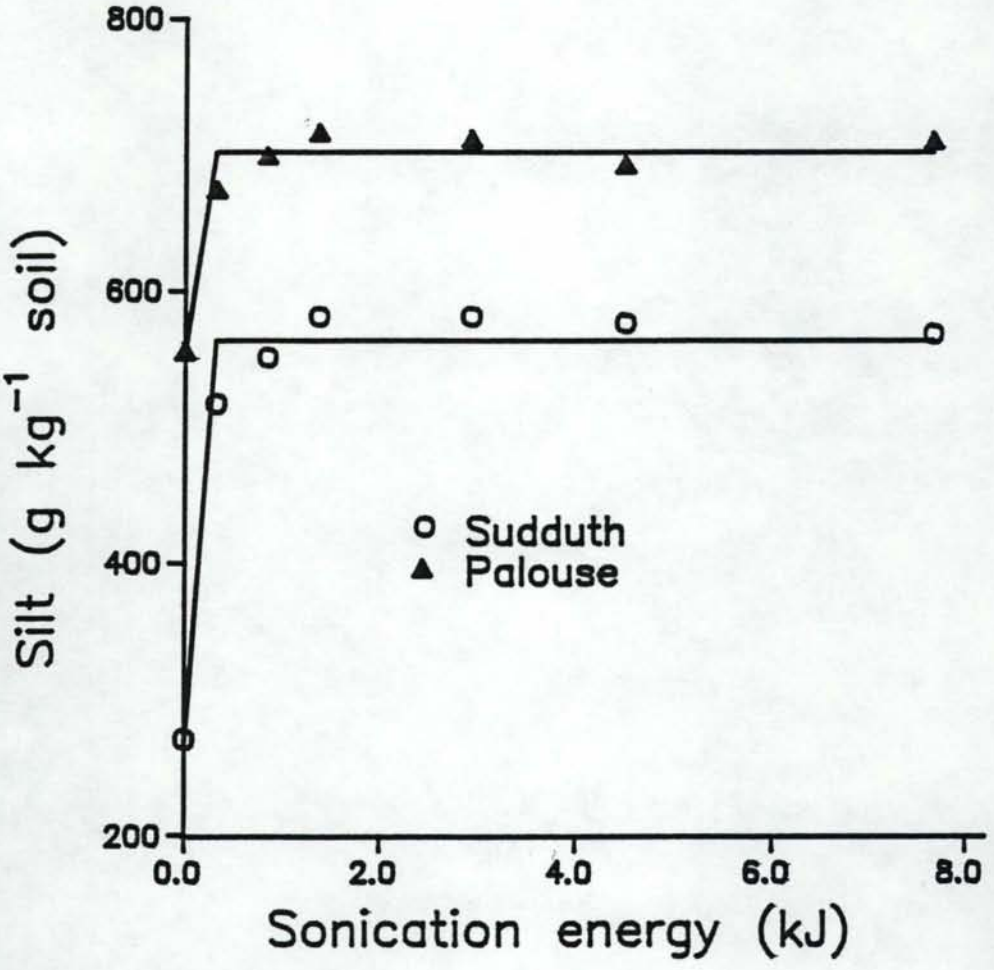

Fig. 1.3. Yields of silt-sized particles from soil after sonication at different energies.

Table 1.3. Models fitted to yields of sand, silt, and clay produced through soil sonication at different energies.

Soil	Sand	Silt	Clay[a]
Sudduth	$Y=318-42.5(\ln x)$ $r^2=0.99$	$Y=264+921x$, $x\leq 0.32$ $Y=564$, $x\geq 0.32$	$Y=56.7+44.2x-3.9x^2$ $r^2=0.90$
Palouse	$Y=177-24.2(\ln x)$ $r^2=0.97$	$Y=555+459x$, $x\leq 0.32$ $Y=702$, $x\geq 0.32$	$Y=67.6+39.5x-3.7x^2$ $r^2=0.88$
Latahco	$Y=248-36.8(\ln x)$ $r^2=0.96$	$Y=434+284x$, $x\leq 0.84$ $Y=674$, $x\geq 0.84$	$Y=44.6+30.8x-2.2x^2$ $r^2=0.95$
Nyssaton	$Y=246-8.6(\ln x)$ $r^2=0.73$	$Y=635+32x$, $X\leq 1.37$ $Y=679$, $x\geq 1.37$	$Y=42.3+14.6x-1.0x^2$ $r^2=0.94$

[a]Includes both coarse (2.0-0.2μm) and medium clay (0.2-0.08μm)

Gregorich et al. (1988; 1989) have more recently used a calibrated probe type sonicator to disperse soil using energies from 100 to 1500 J ml^{-1}. Although the absolute amounts of soil (15 g) and water (75 ml) were different than those used here (10 g soil and 50 ml water), the ratios of soil to water are the same (1:5). Valid comparisons can therefore be made between our data and that reported by Gregorich and co-workers when the values reported in J ml^{-1} are converted to the water volume of 50 ml used in our system. In so doing, it is obvious that the sonication energies of 0.32 to 7.66 kJ as used in the present work were substantially lower than the 5 to 75 kJ used by Gregorich et al. (1988). In spite of this, particle-size yields of Gregorich et al. (1988) followed similar trends and fit the models reported in Table 1.3, with r^2 values of 0.97 and 0.91 for clay and sand, respectively. Yields of silt-sized materials were similar at all sonication energies, apparently reaching a maximum at sonication energies less than 5 kJ as predicted by our data.

Gregorich et al. (1988) argue that silt-sized particle yields do not change with sonication energy, because gains from the sand-sized fraction balance losses to the clay-sized fraction. If this were the case, increased sonication energy would be expected to cause a redistribution in the diameters of the particles contained in the silt-sized fraction. Figure 1.4 shows that no obvious redistribution occurs in the silt-sized fraction of Palouse soil as determined using Coulter Counter data. Statistical comparisons using analysis of covariance confirmed the lack of differences ($P<0.001$) for all soils (data not shown). It therefore seems more likely that the silt-sized fraction

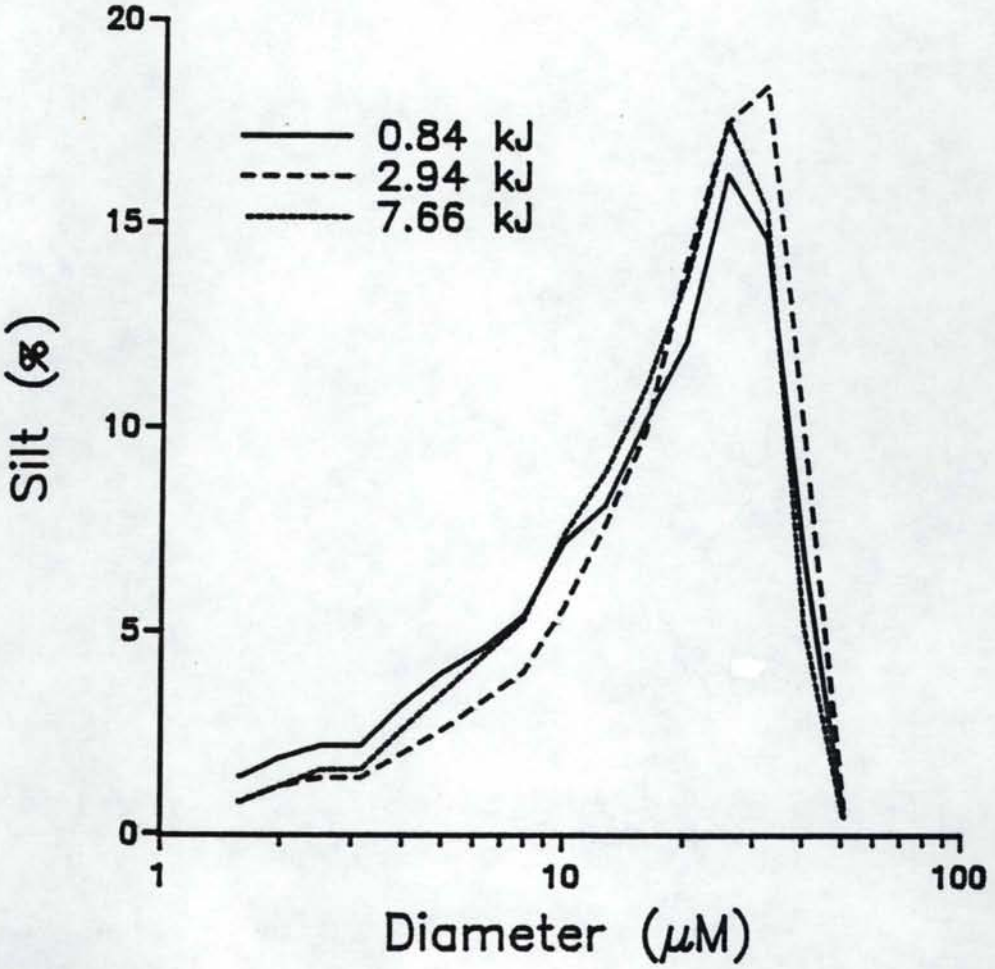

Fig. 1.4. Size distribution of the silt-sized fraction from Palouse soil as determined using Coulter Counter analysis.

represents a more stable assemblage of primary particles than the sand-sized fraction. Contributions to the clay-sized fraction instead come predominantly from the sand-sized fraction and do not pass through an intermediate silt size aggregate.

Quantitative changes in C and N

Total C and N concentrations of the silt-sized fractions show no consistent trends with increased sonication energy (Table 1.4). In contrast, the coarse clay-sized fraction increased in total C concentrations with increased sonication energy, while the medium clay-sized fraction decreased in total C with increased sonication energy. Total N content of the clay-sized fractions showed similar tends in most instances (Table 1.4). Gregorich et al. (1988) did not subdivide the clay fraction, but reported an increase in organic C concentration in the clay-sized fraction with increased sonication, similar to our results for coarse-clay sized materials. The amount of sonication energy is a critical variable in particle size separation if such size fractions are subsequently used to study interactions with natural and synthetic organic compounds. This is true even at relatively low sonication energies less than 7.66 kJ.

Changes that occur in the C concentration of the clay-sized fractions have two possible explanations. Redistribution of the C may result by initial detachment from an organo-mineral complex and subsequent sorption to a different particle size class. Carbon would be redistributed by passing through an intermediate soluble phase. Gregorich et al. (1988) concluded this mechanism to be unlikely since the silt-sized fraction retained such a large proportion of the whole soil organic C even after extended sonication. In addition, losses of

Table 1.4. Total C and N content of silt and clay fractions separated from soil using different sonication energies.

Soil	Sonication energy	Silt		Coarse clay[a]		Medium clay[b]	
		Total C	Total N	Total C	Total N	Total C	Total N
	kJ	g kg^{-1}					
Nyssaton	PSD[c]	0.2	0.8	7.3	2.0	ND[d]	ND
	0.84	16.9	1.4	46.3	3.2	70.4	8.4
	2.94	17.2	1.0	47.5	4.0	67.7	7.4
	7.66	17.2	0.8	48.0	3.6	60.9	4.9
Palouse	PSD	0.9	0.3	6.2	1.4	6.0	1.2
	0.84	12.8	1.5	42.2	4.5	32.0	3.8
	2.94	12.8	1.4	42.7	4.4	31.4	4.0
	7.66	11.4	1.2	43.4	4.5	28.7	3.3
Latahco	PSD	0.9	0.6	13.2	2.8	12.5	2.3
	0.84	31.2	3.0	81.4	7.7	63.8	8.1
	2.94	31.0	3.0	82.2	7.4	59.6	6.8
	7.66	29.0	2.6	84.2	7.6	57.9	6.7
Sudduth	PSD	6.5	1.5	10.3	2.0	15.3	2.8
	0.84	37.2	3.6	43.8	4.8	41.9	5.4
	2.94	39.0	3.6	44.5	5.4	37.4	5.2
	7.66	39.3	3.6	47.0	5.4	37.6	5.0

[a] Includes clay 2.0-0.2μm.

[b] Includes clay 0.2-0.8μm.

[c] Particle size distribution determined with H_2O_2 digestion and chemical dispersion.

[d] Not determined.

soluble C occurring as a result of sonication have been shown to relatively small, amounting to less than 2% of the whole soil C content (Christensen, 1987; Hinds and Lowe, 1980a; Gregorich et al., 1988). If redistribution occurred by way of organic C detachment, larger losses of soluble C would be expected to occur as a result of sonication.

Perhaps a better explanation involves the disruption of aggregates such that the component particle size fractions retain their associated organic matter. Changes in C concentration of the clay-sized fractions result from aggregate disruption and not redistribution of the sorbed organic materials. Avoiding C redistribution among the particle size fractions is a necessary requisite in any procedure designed to obtain artifact-free organo-mineral complexes from whole soils.

Qualitative changes in clay-sized fractions

Attempts to characterize the clay-sized organo-mineral complexes using ^{13}C NMR were unsuccessful, because of high iron concentrations in the samples. Diffuse Reflectance FT-IR (DRIFT) was used as alternative technique to determine qualitative differences in the clay-sized fractions. Infrared spectra of inorganic compounds and clays have been successfully determined using DRIFT (Bowen et al., 1989; Iwaoka et al., 1985).

No obvious differences occurred in spectra of the coarse clay-sized fractions obtained with different sonication energies (Fig. 1.5), nor did sonication alter the spectra of medium clay-sized fractions from Nyssaton and Palouse soils (data not shown). In contrast, spectra of the medium clay-sized materials from Latahco and Sudduth soils were altered by increased sonication (Figs. 1.6,1.7). The most dramatic changes, including peak shifts and amplitude differences, occur from

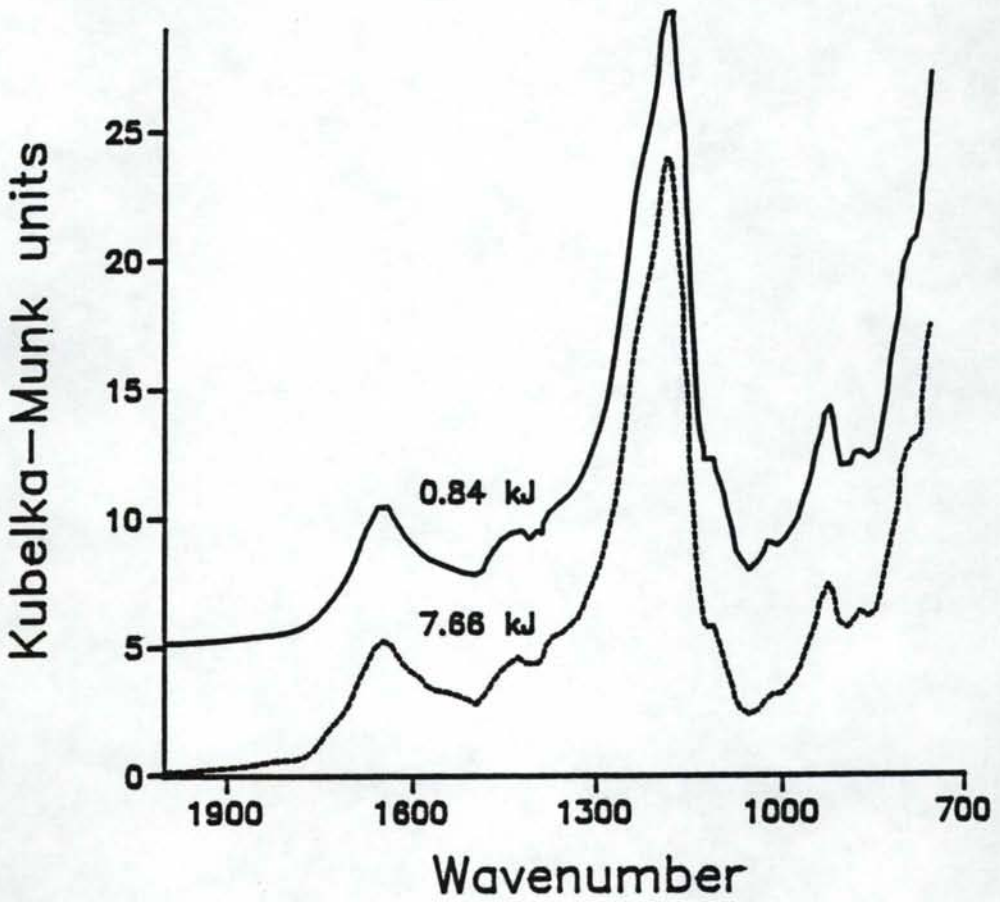

Fig. 1.5. DRIFT spectra of coarse clay separated from Sudduth soil after 0.84 or 7.66 kJ of sonication energy.

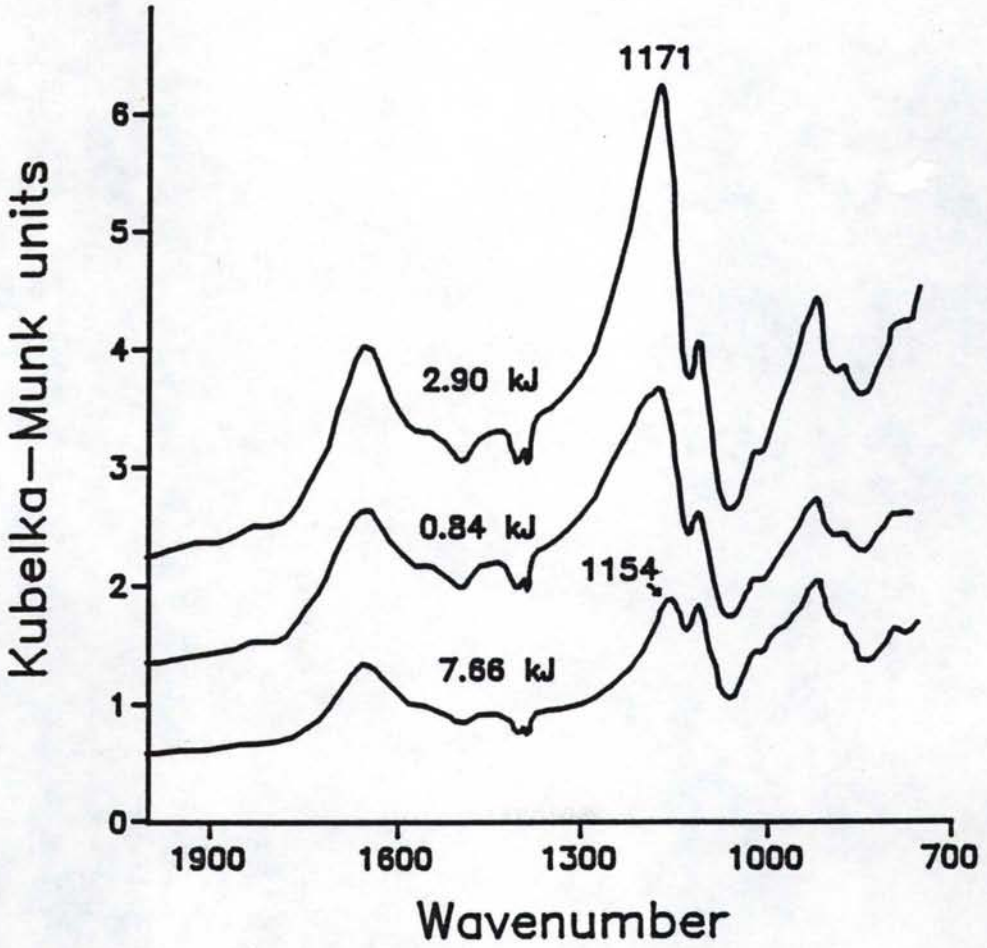

Fig. 1.6. DRIFT spectra of medium clay separated from Sudduth soil after different sonication energies.

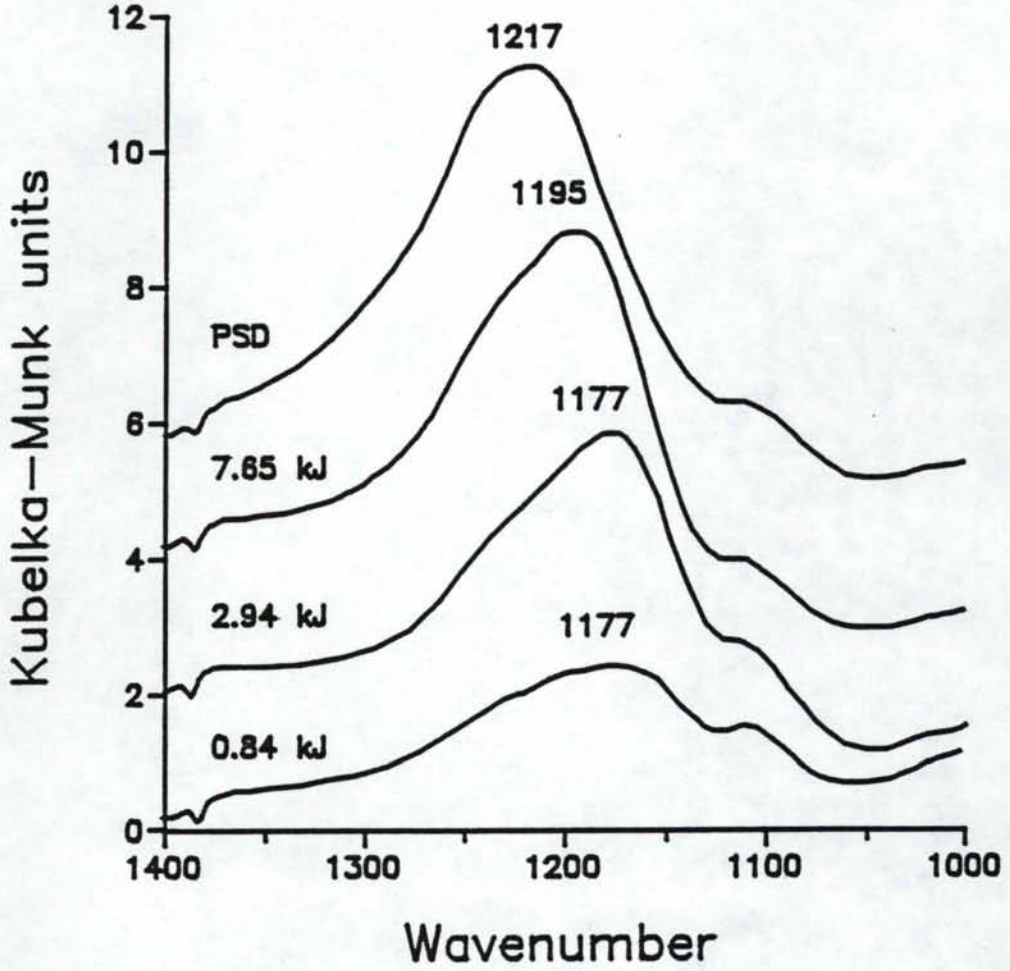

Fig. 1.7. DRIFT spectra of medium clay separated from Latahco soil after different sonication energies.

1100 to 1300 cm^{-1} and therefore in the region indicative of silica type minerals (van der Marel and Beutelspacher, 1976).

It seems unlikely that sonication altered the clay minerals themselves. It has been determined that structural alterations only occur when clay minerals are sonicated in the absence of organic matter and subjected to high energies (North, 1971). This observation is supported by recent studies in which sonication energies of 75 kJ did not alter clay surface areas (Gregorich et al., 1988) and 23 kJ did not destroy primary sand- and silt-sized glass shards or imogolite threads in the clay fraction (Hunter and Busacca, 1989). Hinds and Lowe (1980a) have reported however, that sonication resulted in mineral dissolution and the release of significant quantities of Fe, Al, and Si. More recent evidence suggests that elevated concentrations of these elements occurred as a result of an incomplete separation of fine suspended particles from the supernatant prior to elemental analysis by atomic absorption spectroscopy (Escudey et al., 1989).

Changes in the spectra thus most likely result from alteration of the organic matter associated with organo-mineral complex. The exact nature of these changes is impossible to determine based only upon DRIFT data, but does demonstrate that sonication qualitatively alters organo-mineral complexes even at relatively low sonication energies of 0.84 to 7.66 kJ. It is therefore suggested that a standard sonication energy between 3 and 5 kJ and a soil to water ratio of 1 to 5 be used in order to obtain reasonable particle size yields and minimize qualitative changes in the fractionated organo-mineral complexes.

NIRS DETERMINATION OF TOTAL CARBON AND NITROGEN IN SILT AND CLAY SIZE FRACTIONS

M.J. Morra, M.H. Hall, and L.L Freeborn

Abstract

A non-destructive method to determine total C and N concentrations in soil size fractions is desirable when limited sample is available. Near Infrared Reflectance Spectroscopy (NIRS) was used to determine the total C and N concentrations in silt (50.0-2.0 μm) and coarse clay (2.0-0.2 μm) separated from twelve surface soils by regressing the diffuse reflectance of near infrared radiation with constituent concentrations determined using combustion techniques. The correlation coefficients (R^2) of NIRS predicted and combustion values were 0.93 and 0.89, and the standard errors associated with NIRS predictions were 6.2 and 0.6 g kg^{-1} soil for total C and N, respectively. Inclusion of only silt samples in equation development improved the accuracy of NIRS prediction, resulting in R^2 values of 0.96 and 0.94 for total C and N, respectively. Coefficients of variation [CV = (standard error of performance / mean of the combustion procedure) x 100] for validation sample sets ranged from 14 to 19% which is within the range of what is considered acceptable for the determination of inorganic elements in plant tissues. We conclude that NIRS can be used to non-destructively predict C and N concentrations in soil size fractions and that accuracy of this analytical method can be improved by reducing variability in the calibration sample set.

Introduction

Near infrared reflectance spectroscopy (NIRS) has become widely accepted as a non-destructive method for quality analysis of forage material (Shenk et al., 1981; Wetzel, 1983; Windham et al., 1988; Marten et al., 1989), but has applications as diverse as quantifying blood meal size in live female mosquitoes (Hall et al., 1990). Bowers and Hanks (1965) made some of the earliest infrared refectance measurements of soils and found that the spectra were influenced by moisture content, organic matter, and particle size. More recent investigations demonstrated the potential use of NIRS for non-destructive analysis of soil organic C, total N, and moisture content (Dalal and Henry, 1986; Krishnan et al., 1980).

NIRS makes use of diffuse reflectance to quantify constituents within a sample. Each constituent of a complex organic mixture has unique absorption properties in the near infrared region of the spectrum (700 to 2500 nm) due to stretching and bending vibrations of molecular bonds between elements. Fundamental absorption bands are located at energy levels which allow the molecule to rise to higher vibrational states. These bands occur in the mid infrared region and their overtones (1/2, 1/3, 1/4, ..., of the wavelength of the fundamental band) occur in the near infrared region. Overtones are specific to each constituent and are more sensitive to changes in the chemical composition of the absorbing molecule than fundamental absorption bands of the same vibration (Wetzel, 1983). Thus the diffuse reflectance properties of the near infrared spectrum of a sample can be correlated to changes in the chemical composition of a sample measured by other means.

Our objective was to determine the utility of NIRS to predict total C and N concentrations in particle size fractions separated from soils. Yields of soil size fractions are in many instances quite low, and the ability to non-destructively quantify total C and N concentrations is of interest in order to preserve as much of the sample as possible for further experimentation.

Materials and Methods

Twelve soils were selected to obtain a range in pH, organic carbon, free carbonates, and texture (Table 2.1). Surface soil samples (0-35 cm) were collected, air-dried, and sieved (2mm). Analyses were conducted using the following methods: pH by glass electrode (1:1 soil to water), organic C by the Walkley-Black method (Nelson and Sommers, 1982), total C and N by Dumas combustion (LECO CHN-600 Determinator, St. Joseph, MI), and particle-size distribution by the hydrometer method (Day, 1956).

Silt (50.0-2.0 μm) and coarse clay (2.0-0.2 μm) fractions were separated from each of the soils using two methods. Particle size fractions with low concentrations of C and N were obtained using standard methods in which free carbonates and organic matter are removed prior to dispersion with sodium hexametaphosphate (Jackson, 1956). In the second method, particle size fractions with relatively high concentrations of C and N were obtained using ultrasonic dispersion on otherwise untreated soils. All dispersion treatments and separations were replicated four times. Carbon and N were determined for individual replicates of all silt samples. Replicates of coarse clay were combined

Table 2.1. Characteristics of soils used in isolation of coarse clay and silt size fractions.

Soil			Total	Organic	Total		
Series	Subgroup	pH	carbon	carbon	nitrogen	Clay	Sand
			----------	----------	g kg^{-1}	----------	----------
Unnamed	Pachic Calcixerolls	8.0	50.4	26.3	2.6	203	136
Hat	Typic Xerumbrepts	5.5	42.0	42.0	3.4	236	447
Morton	Typic Cryaquolls	7.4	80.4	63.5	6.0	383	139
Unnamed	Ultic Haploxeralfs	5.0	32.4	32.4	1.6	175	296
Fenn	Chromic Pelloxererts	5.9	28.0	28.0	2.0	343	193
Sudduth	Argic Pachic Cryoboralls	5.6	47.5	44.2	3.2	323	270
Melton	Humic Cryaquepts	5.8	28.0	28.0	2.3	53	380
Nyssaton	Xerollic Calciorthids	6.9	20.2	8.5	0.8	32	294
Feltham	Xeric Torriorthents	6.3	8.2	6.3	0.8	40	830
Palouse	Pachic Ultic Haploxerolls	5.7	19.5	19.2	1.6	203	167
Latahco	Argiaquic Xeric Argialbolls	6.1	41.0	41.0	3.9	159	121
Portneuf	Durixerollic Calciorthids	7.3	15.6	ND[a]	1.7	157	48

[a]Not determined.

when the sample size was insufficient to fill the NIRS sample cell. The total number of silt and clay samples were 56 and 28, respectively.

Dispersion by sonication was performed by placing 10 g soil and 50 mL of water into a 100 mL plastic centrifuge tube, stirring with a glass rod, and applying 0.32, 0.84, 1.37, 2.94, 4.51, or 7.66 kJ of energy using a Biosonic III probe type sonifier (Bronwill Scientific, Rochester, NY). Time of energy application required to achieve the total input energies above ranged from 0 to 300 s, with energy output from the probe tip calibrated using the methods of North (1976). Separation of the silt and coarse clay was completed using the methods of Jackson (1956), except that no hexametaphosphate was added. All samples were freeze dried after separation and ground using a mortar and pestle. Total C and N in each sample was determined using a LECO CHN-600 Determinator (St. Joseph, MI).

Near infrared reflectance measurements were made with a Pacific Scientific Neotec 6250 Scanning Reflectance Monochromator (Silver Spring, MD). Each sample was packed into a sample cell having a quartz-glass cover, and reflectance (R) measurements (log 1/R) of monochromatic light were completed from 1100 to 2500 nm, averaged over 64 scans, and recorded at 2-nm intervals.

The spectroscopic data were related to the combustion determined total C and N concentrations using modified stepwise linear regression. Every fifth sample (n = 16) was reserved for use in validation following equation development, while the remaining samples were used for calibration (n = 68). The calibration procedure consisted of a computer search for the wavelengths that gave the best linear relationship of total C and N concentration with a function (first or second order

derivative) of the reflectance data. A maximum of eight wavelengths per transformation were correlated to combustion determined concentrations of the elements. The best predictive equation was chosen as the equation with the lowest standard error of calibration (SEC) and fewest wavelengths, with no wavelengths having F statistics < 10 or regression coefficient terms > 14 000. Validation of the selected equations ability to predict total C and N was completed using the 16 reserved samples. More complete descriptions of the currently accepted techniques for equation selection and validation are available (Abrams et al., 1987; Westerhaus, 1989a; Westerhaus, 1989b; Windham et al., 1989).

NIRS prediction of total C and N concentrations in the silt samples alone was performed to evaluate NIRS performance with a more homogeneous sample set. NIRS analyses were performed as previously described using 45 samples for calibration and 11 samples for validation of the NIRS predictive equation. The calibration was limited to a maximum of five wavelengths.

Statistical evaluation of calibration and validation procedures was performed using parameters commonly accepted in NIRS analysis (Clark et al., 1989; Windham et al., 1989). SEC, standard error of prediction (SEP), and coefficient of variation (CV) were calculated according to the following equations:

$$SEC = (\text{mean square error})^{0.5}$$

$$SEP = \{[(A - B)^2]/n\}^{0.5} - (\text{bias}/n)$$

$$CV = (SEP/\text{mean of combustion procedure}) \times 100$$

where A = NIRS values, B = combustion values, n = number of samples, and bias = NIRS mean minus the combustion mean.

Results and Discussion

It was our purpose to include soils with a wide range in total C and N concentrations as well as having potential qualitative differences in these elements (Table 2.1). The range in concentrations was extended by digesting a subset of these samples with H_2O_2. In this manner the calibration sample sets represent what are considered to be extreme cases for developing predictive NIRS equations.

Correlations were developed for both elements using soil fractions with C and N concentrations of 0.5 to 90.2 g and 0.2 to 7.5 g kg^{-1} soil, respectively (Table 2.2). Six wavelengths with a first order derivative math treatment produced the best equation for NIRS analysis of the elements when both silt and coarse clay fractions were included. Krishnan et al. (1980) used various reflectance transformations and found the best correlation with soil organic matter to occur with either 1136 and 1398 nm or 1080 and 2212 nm. Only 2212 nm corresponds to similar wavelengths selected for total C analysis of soil particle size fractions (Table 2.2). Dalal and Henry (1986) used log 1/R values and chose 1744, 1870, and 2052 nm to be most acceptable for NIRS analysis of organic C and 1702, 1870, and 2052 nm for total N in whole soils. Little agreement between the present and past research occurs with respect to optimum wavelengths and most appropriate transformation of the reflectance data for analysis of C and N in soils.

The R^2 values for the combined silt and coarse clay calibration sample set were 0.93 and 0.89 for C and N, respectively (Table 2.2). The R^2 values of calibration equations used in the analysis of crude protein in forages usually exceed 0.90, while the R^2 values used to determine Ca, P, K, and Mg concentrations in plant tissues are lower,

Table 2.2. Equation calibration statistics for total C and N concentrations in soil size fractions.

Size fraction	Element	Combustion Mean	Combustion Range	SEC[a]	R^2	Math trt[b]	Wavelengths[c]
		------- g kg^{-1} ------					nm
silt + coarse clay	C	28.6	0.5-90.2	6.2	0.93	1	2426,1736,2210,2032, 2250,2170
	N	2.8	0.2- 7.5	0.6	0.89	1	2432,2176,1446,2038, 1920,2136
silt	C	24.0	0.6-78.0	4.1	0.96	1	2206,2226,1766,2346, 2246
	N	2.3	0.2- 6.4	0.4	0.94	2	1726,1646,1246,2366, 1826

[a]Standard Error of Calibration.

[b]Math treatment: 1 = first derivative; 2 = second derivative.

[c]Wavelengths used in the equation in order of decreasing contribution.

ranging from 0.73 to 0.88 (Clark et al., 1987). The determination of organic C and total N in whole soils produced R^2 values of approximately 0.86 (Dalal and Henry, 1986; Krishman et al., 1980).

Clark et al. (1989) determined the ability of NIRS to predict inorganic trace elements in forages and concluded that the measurement of quality parameters in forages (e.g. protein, fat, oil) differs from elemental determination in that there is a direct relationship between the quality parameter of interest and the wavelengths of the reflectance measurements selected, while in inorganic analysis the reflectance measurement is based on an indirect correlation of unknown origin. The analysis of C and N in soil size fractions represents a combination of wavelengths representing absorbances of identifiable C or N bonds as well as unexplainable correlations. Intermediate R^2 values between those found for quality parameters of forages and inorganic elements in plant tissues are thus expected in the determination of C and N concentrations in soil size fractions.

Accuracy was increased by including only silt in equation development and validation as shown by both R^2 and SEC values (Table 2). Increased accuracy may result from decreased variability in particle size, as it relates to matrix effects occurring in the NIRS method, or may be a function of increased similarity in the chemical composition of the C and N pools. Particle size has been shown to influence NIRS spectra (Krishnan et al., 1980), especially when particle diameters are less than 400 mm (Bowers and Hanks, 1965). Mineralogical differences, as are most likely present with our soils, have also been shown to alter infrared reflectance measurements (Bowers and Hanks, 1965).

Validation of both sample sets, silt plus coarse clay and silt only, showed similar means and SD between the combustion determined and the NIRS predicted C and N concentrations (Table 2.3). SEP values have most frequently been used to evaluate the accuracy of the NIRS predictive equation in forage analysis. SEP values decreased when only silt was included in the calibration and validation sample sets as compared to silt plus coarse clay.

Comparison of SEP values determined here with results of other investigators is misleading, because SEP values are dependent upon the amount of variation in the chemical analysis data. Instead, Clark et al. (1987; 1989) proposed the use of CV values as a means to facilitate the evaluation of equation performance. Quality parameters of plant tissues generally exhibit CV values less than 10% (Marten et al., 1984; Marten et al., 1983), whereas CV values less than 20% are considered acceptable for the prediction of inorganic constituents in forages (Clark et al., 1987; Clark et al., 1989). Validation sample sets for both silt plus coarse clay and silt only have CV values ranging from 14 to 19% for total C and N (Table 2.3). Dalal and Henry (1986) did not report CV values for the determination of organic C and N in whole soils and insufficient data is presented to allow for an exact calculation. However, approximate CV values for organic C and total N range from 16 to 38% even though the samples included a much narrower range in organic C (2.7-25.1 g kg^{-1}) and total N (0.19-2.26 g kg^{-1}) than the sample sets used here.

A graphical comparison of combustion determined and NIRS predicted total C concentrations for the silt size fraction is shown in Fig. 2.1 as a representative validation sample set. The more accurate the

Table 2.3. Validation statistics of NIRS predicted and combustion determined total C and N concentrations in soil size fractions.

Size fraction	Element	Combustion		NIRS			
		Mean	SD	Mean	SD	SEP[a]	CV[b]
		g kg^{-1}					%
silt + coarse clay	C	30.8	24.2	32.3	22.3	5.9	19
	N	3.1	1.9	3.1	1.8	0.6	19
silt	C	22.6	22.0	23.0	22.3	3.2	14
	N	2.1	1.6	2.5	1.6	0.4	17

[a]Standard Error of Prediction

[b]Coefficient of Variation

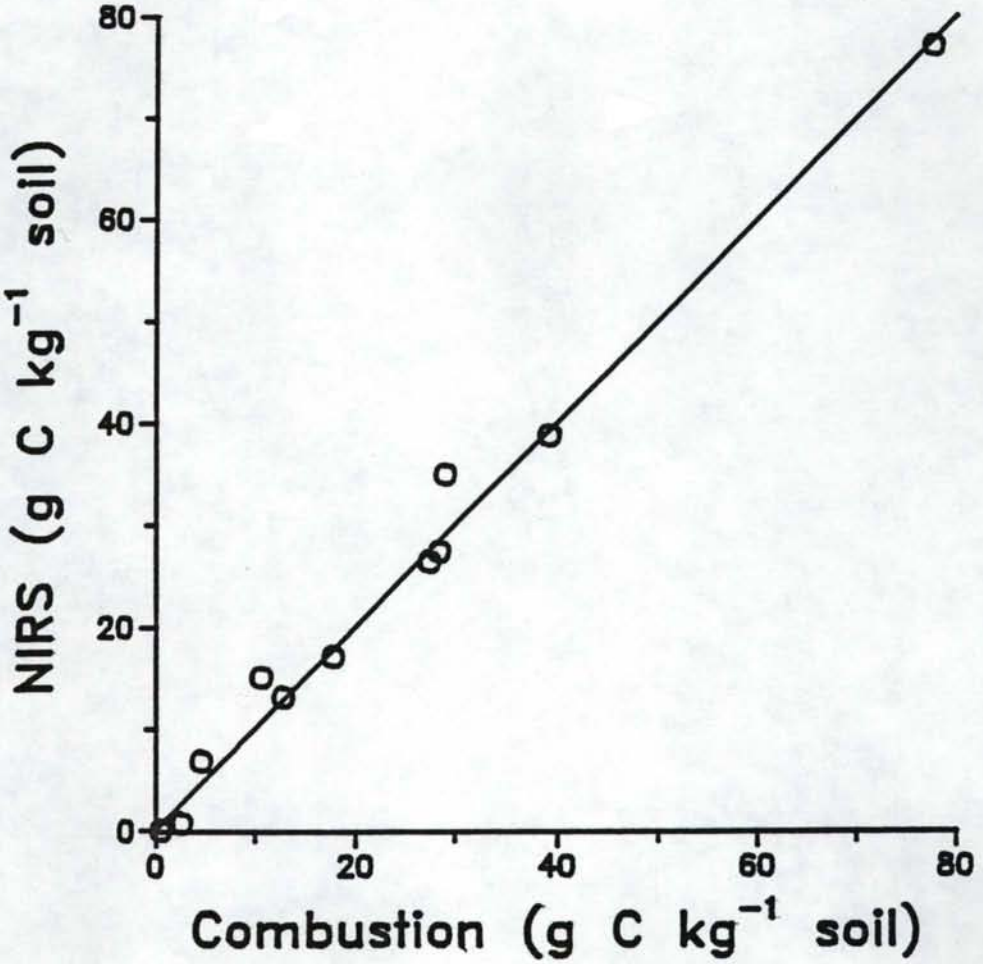

Fig. 2.1. Validation of NIRS predicted with combustion determined total C concentrations in silt size fractions. Solid line represents 1:1 agreement between the methods.

predictive equation, the more closely all points cluster near the theoretical 1:1 correspondence shown by the solid line. Other validation sample sets display more scatter about this line (data not shown), resulting in higher CV values.

The non-destructive determination of C and N in soil fractions is most critical when limited sample is available and it is necessary to preserve as much of the sample as possible for further analyses. This is often the case when clay less than 0.2 μm is the subject of interest, because of the low yields obtained from soils. The NIRS sample holder used in this research has a reflectance surface area of 3.6 cm^2. The minimum sample size, assuming a sample depth of 4 mm and bulk density of 1.3 g cm^3, is approximately 2 g. Sample cells requiring less sample than used in this work are commercially available. The use of smaller sample cells will greatly increase the utility of this technique.

The necessity of having a relatively large sample set to perform the calibration procedure also limits the value of NIRS in the quantification of C and N in soil size fractions. Indeed, the necessity of using a defined or closed sample population for NIRS analysis of any constituent is an inherent limitation of the procedure. The feasibility of using broad-based calibrations that can be transferred to different instruments has been explored in forage quality analyses (Abrams et al., 1987), but was not possible here because of the necessity for a greater number of samples. Present results indicate that NIRS is a non-destructive technique capable of predicting total C and N concentrations in soil size fractions and that improvements to increase the applicability of the method are possible.

FLUORESCENCE CHARACTERISTICS OF DIFENZOQUAT

R. von Wandruszka, W.D. Edwards, M.M. Puchalski, and M.J. Morra

Abstract

Difenzoquat is identified as a potentially useful fluorescence probe. Its fluorescence excitation spectrum shows significant concentration-dependent variations not found in the absorption and fluorescence emission spectra. The effects are ascribed to association phenomena that are unaffected by ionic strength and anionic/non-ionic detergents, but strongly promoted by cationic micelles. INDO calculations account for the features of the monomer excitation spectrum, but do not explain concentration dependent behavior.

Introduction

1,2-Dimethyl-3,5-diphenylpyrazolium methylsulfate, commonly known as difenzoquat, is a widely used herbicide with fungicidal properties:

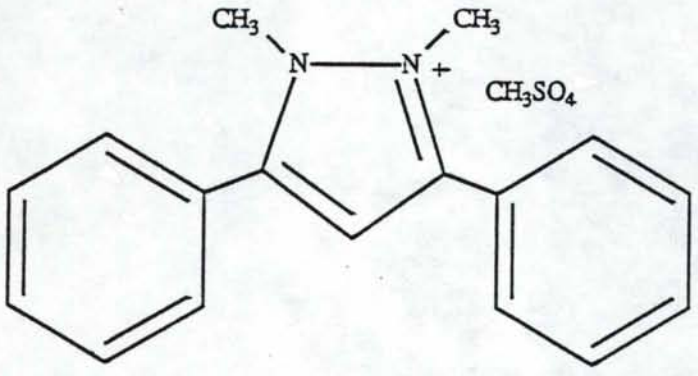

In the soil, difenzoquat is fairly readily demethylated photolytically to the relatively volatile monomethyl pyrazole (WSSA, 1983). However, aqueous solutions retain their spectroscopic integrity for days and in the dark for weeks.

Difenzoquat is of interest not only because of environmental considerations, but also because it is potentially a useful fluorescent probe. It is a strong emitter with relatively compact molecular dimensions, containing an ionic group that can be used as a reactive site to anchor the probe to a receptor. These properties suggest applications of difenzoquat in fluorescence studies of micro-organized systems such as micelles and membranes.

In the present study it was found that difenzoquat has unusual fluorescence characteristics, especially with regard to its excitation and absorption spectra.

Materials and Methods

Difenzoquat (98.1%) was obtained from American Cyanamid Corp., under the trade name AVENGE. It was recrystallized from isopropanol and purified by cold finger sublimation. [The compound is also available from Riedel-deHaen under the Pestanal brand name, distributed by Fisher Scientific.] Cetyltrimethyl-ammonium bromide (CTAB) and sodium lauryl sulfate (SLS) were obtained from Sigma and purified by recrystallization from absolute ethanol. The following were used without further purification: polyoxyethylene 23-lauryl ether (Brij 35) (Sigma), n-hexane (EM Sciences), and potassium sulfate RG (Baker). Distilled deionized water, treated with a micropore filter to 18 MΩ cm resistivity, was used throughout.

Difenzoquat solutions in n-hexane were prepared by sonication for 30 min and subsequent filtering through glass wool. Detergent solutions were heated and sonicated until no trace of turbidity remained. Fluorescence spectra were recorded with a Perkin-Elmer MPF 66 Spectrofluorimeter equipped with a thermostated sample compartment. The instrument provides corrected excitation spectra, through the use of a built-in Rhodamine 101 quantum counter. Fluorescence-free quartz cells were used and solution temperatures were held at 25°C. Blank subtraction of all fluorescence spectra was carried out through instrument software. Absorption spectra were taken with a Perkin-Elmer Lambda 4C Spectrophotometer.

Surface tension and conductivity measurements were obtained with a Cenco DuNouy Interfacial Tensiometer and a Yellow Springs Instruments Model 32 Conductance Meter, respectively.

Theoretical Methods

Semi-empirical (INDO) quantum mechanical calculations, based on the methods of Ridley and Zerner (Ridley and Zerner, 1973, Ridley and Zerner, 1976), were used in this investigation. The starting geometry of difenzoquat was derived from the MM2 molecular mechanics optimization structure and was refined by the gradient based optimization method of Head and Zerner (Head and Zerner, 1985). The optimized geometry was used in all subsequent calculations. The original Pople, Santry and Segal parameterization (Pople et al., 1976) was used for the ground state calculations.

In addition to the ground state calculations, a series of Configuration Interaction (CI) calculations (Bacon and Zerner, 1979)

were carried out at selected rotation angles. They were performed with INDO/S spectroscopic parameters and excited states were generated from single electron excitations only. From these CI calculations, the transition energy between ground and excited states was obtained as a function of the phenyl group rotation angles. Transition moments were calculated using the dipole length operator and keeping all one-center charge and polarization terms. All calculations were run on a Hewlett Packard 9000/350 workstation, a component of the Computational Facility for Theoretical Chemistry at the University of Idaho.

Results

Difenzoquat shows strong fluorescence emission, with excitation maxima at 226 and 280 nm, and an emission maximum at 373 nm in water. As expected, the ionic nature of this fluorophore results in a hypsochromic emission shift with decreasing solvent polarity, because the ion interacts more strongly with polar media. In aqueous solution, the position of the fluorescence emission band is unaffected by the difenzoquat concentration or by the excitation wavelength chosen.

However, the corrected excitation spectrum varies strongly with concentration and depends in some instances on the presence of ionic species in solution; these effects are not observed in the difenzoquat absorption spectrum. Fig. 3.1 shows the changes in the excitation spectrum--the long-wavelength peak shifts bathochromically with increasing concentration, while the short-wavelength peak shifts slightly hypsochromically. Only at very low difenzoquat concentration (6.9×10^{-6} M) does the excitation spectrum resemble the absorption spectrum shown in Fig. 3.2. This effect depends on the difenzoquat

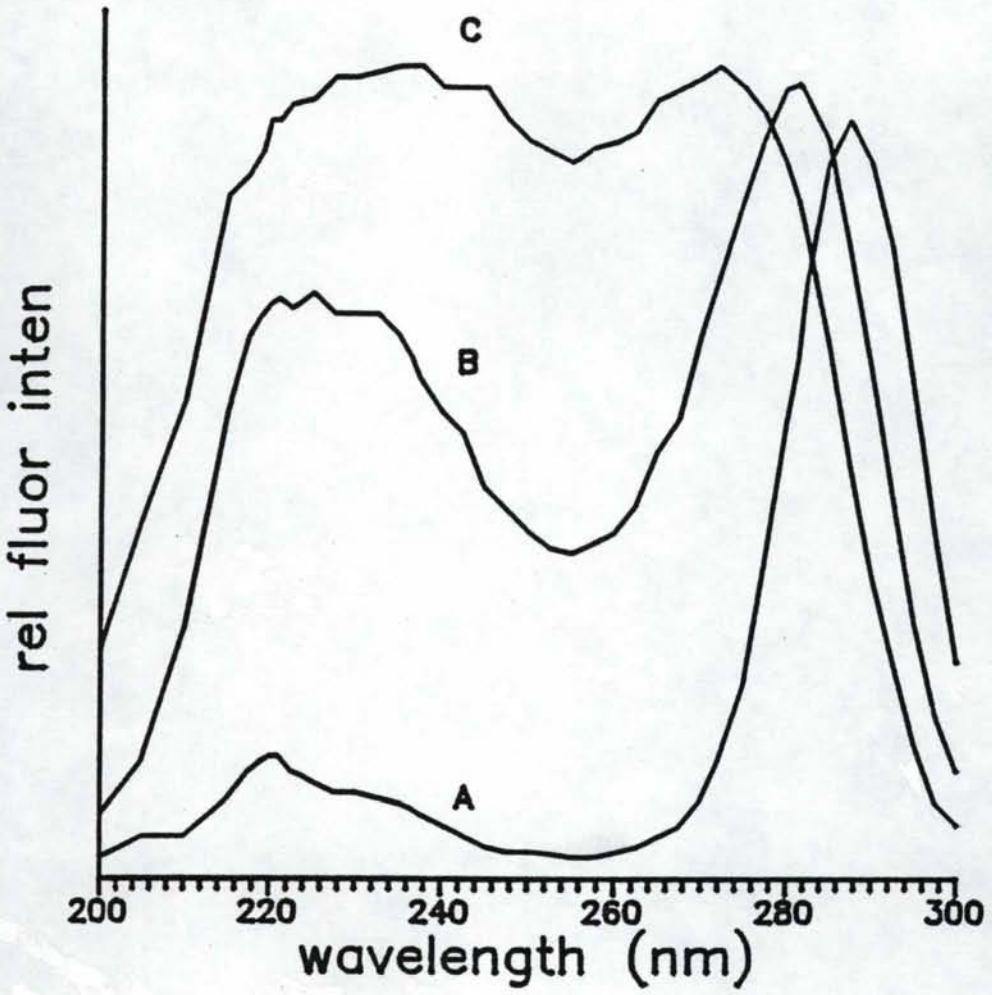

Fig. 3.1. Fluorescence excitation spectra of difenzoquat at different concentrations: (A) 3.5 x 10^{-4} M; (B) 1.4 x 10^{-4} M; (C) 6.9 x 10^{-5} M.

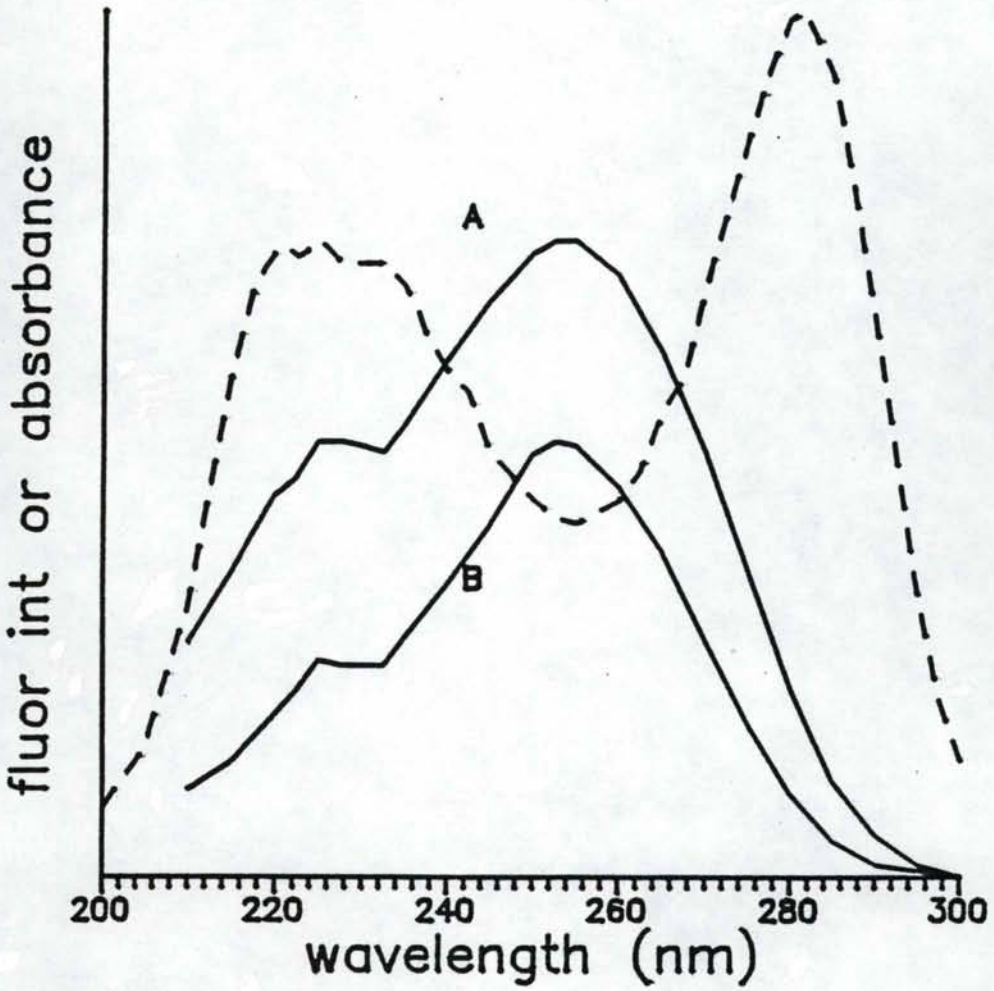

Fig. 3.2. (A) Fluorescence excitation spectrum of 6.9 x 10^{-6} M difenzoquat; (B) absorption spectrum of 1.4 x 10^{-4} M difenzoquat; dashed line: excitation spectrum of 1.4 x 10^{-4} M difenzoquat.

concentration only and not on the exact nature of the aqueous medium--it occurs virtually to the same extent in pure water, 0.1 M K_2SO_4, and micellar solutions of SLS (anionic detergent), CTAB (cationic detergent), and Brij 35 (anionic detergent). The absorption spectrum has the short-wavelength band found in the excitation spectrum, but the long-wavelength peak is located at 253 nm, and remains more or less in the same position at all difenzoquat concentrations, while the excitation maximum shifts as far as 290 nm. The excitation spectrum of difenzoquat dissolved in n-hexane (Fig. 3.3) is very similar to the absorption spectrum in aqueous solution.

The relative intensities of the long- and short-wavelength excitation peaks vary with concentration, and, importantly, also with the nature of the aqueous medium. This is summarized in Table 3.1, where I_1/I_2 refers to the ratio of the long-wavelength to short-wavelength peak heights. This ratio is a relative measure of the populations of the species excited at these wavelengths.

It is immediately obvious that a difenzoquat concentration increase not only shifts the long-wavelength excitation peak bathochromically, but also increases its intensity. While the two bands are of approximately equal height at 6.9×10^{-5} M, the long-wavelength band becomes about 5 times as intense at 3.5×10^{-4} M. An increase in ionic strength and the presence of SLS and Brij enhance the effect slightly. However, micellar CTAB has a major influence: the long-wavelength peak becomes more than 12 times as high as the short-wavelength peak.

This exceptional effect of CTAB is only observed with micellar solutions. In premicellar CTAB (1.0×10^{-4} M) the enhancement of the long-wavelength peak is similar to that obtained with the other

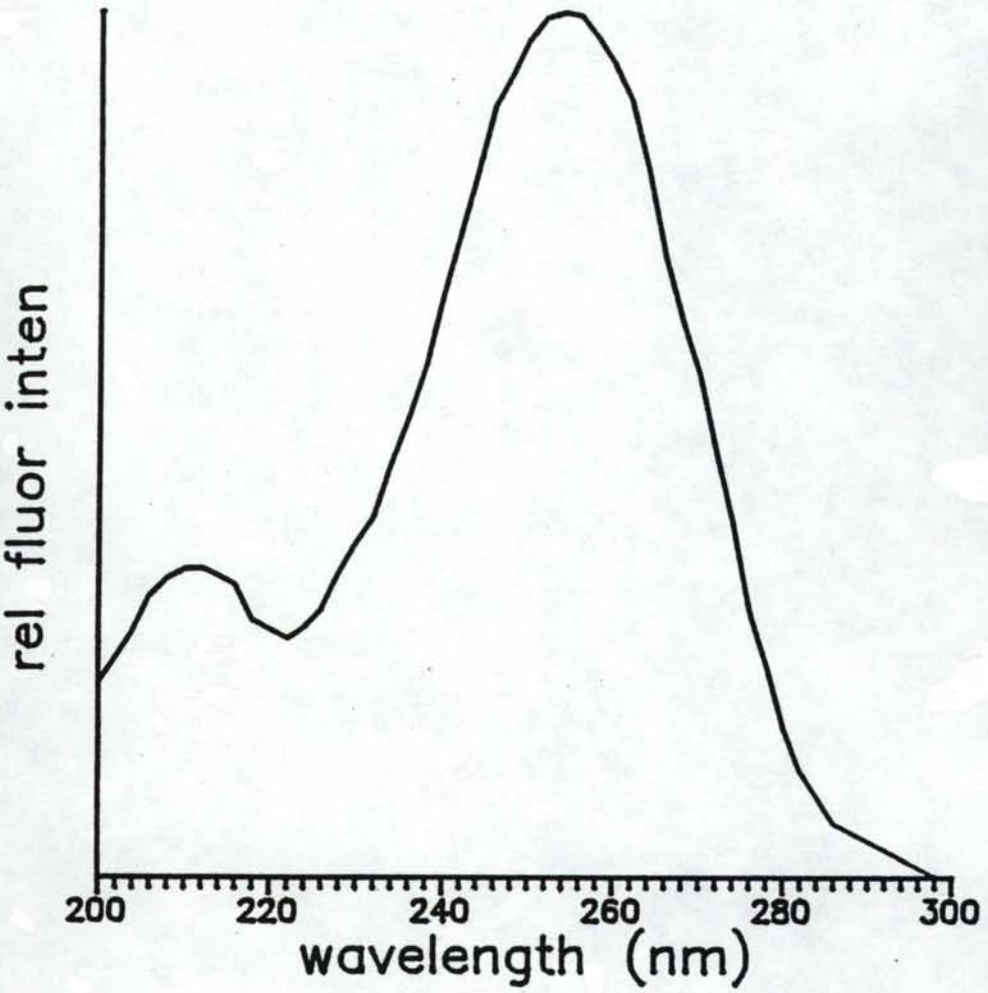

Fig. 3.3 Fluorescence excitation spectrum of difenzoquat in n-hexane (sat).

Table 3.1. Variation of long-wavelength/short-wavelength excitation band ratio with difenzoquat concentration and solution conditions.

Difenzoquat conc (M)	Other solute conc (M)	I_1/I_2
6.9×10^{-5}	-	0.97
1.4×10^{-4}	-	1.27
3.5×10^{-4}	-	4.87
	K_2SO_4	
6.9×10^{-4}	2.9×10^{-3}	0.99
1.4×10^{-5}	2.9×10^{-3}	1.33
3.5×10^{-4}	2.9×10^{-3}	5.49
6.9×10^{-5}	1.0×10^{-2}	0.98
1.4×10^{-5}	1.0×10^{-2}	1.30
3.5×10^{-4}	1.0×10^{-2}	6.31
	SLS	
6.9×10^{-5}	1.0×10^{-1}	1.10
1.4×10^{-5}	1.0×10^{-1}	1.30
3.5×10^{-4}	1.0×10^{-1}	6.31
	CTAB	
6.9×10^{-5}	1.0×10^{-1}	1.09
1.4×10^{-5}	1.0×10^{-1}	1.63
3.5×10^{-4}	1.0×10^{-1}	12.37
	Brij 35	
6.9×10^{-5}	1.0×10^{-1}	1.02
1.4×10^{-5}	1.0×10^{-1}	1.42
3.5×10^{-4}	1.0×10^{-1}	5.89

solutions listed. Moreover, there is no significant influence of micellar CTAB on the absorption spectrum of difenzoquat.

INDO optimized geometry calculations have been remarkably successful in predicting the UV/visible spectra of a wide variety of aromatic molecules (Edwards and Zerner, 1983; Zerner et al., 1980). For difenzoquat they indicate that the phenyl rings are nearly coplanar with the central ring. The ground state energy of the system was also calculated as a function of the symmetric rotation of these phenyl groups, and the results are listed in the first row of Table 3.2. The barrier to simultaneous rotation of the phenyl groups was calculated to be 3.3 kcal/mol.

Since the extent of delocalization can have a profound effect on electronic spectra, the nine lowest excited states were calculated with INDO/S for all rotational geometries. The energies of these states, along with oscillator strengths, are included in Table 3.2. From these results, the rotational barrier for the first excited state was estimated to be 11 kcal/mol.

Surface tension measurements of difenzoquat solutions in the range 6.9×10^{-6} M to 3.5×10^{-4} M showed only a small, gradual decrease with increasing concentration. The molar conductivities of the solutions varied similarly.

Table 3.2. Ground and excited state energies (in 1,000 cm^{-1}) as a function of phenyl group rotation angle. Oscillator strengths are shown in parentheses.

Angle	0.0	15.0	30.0	45.0	60.0	75.0	90.0
State							
0	0.0	0.04	0.06	0.31	0.70	1.00	1.14
1	29.6 (1.10)	29.9 (1.09)	30.7 (1.02)	31.9 (0.90)	33.4 (0.68)	33.7 (0.04)	33.6 (0.01)
2	33.9 (0.27)	33.9 (0.25)	34.0 (0.21)	33.9 (0.15)	33.9 (0.09)	35.0 (0.33)	35.8 (0.00)
3	34.4	34.5	34.7	35.2	35.9	36.7	37.5
4	34.5	34.6	34.9	35.4	36.2	37.0	37.5
5	40.7 (0.28)	40.7 (0.27)	40.9 (0.16)	41.1 (0.03)	40.3 (0.00)	39.2 (0.09)	38.3 (0.33)
6	42.4 (0.03)	42.2 (0.03)	41.9 (0.03)	41.3 (0.03)	40.6 (0.03)	39.4 (0.10)	38.8 (0.00)
7	42.4 (0.03)	42.4 (0.03)	42.1 (0.03)	41.6 (0.03)	40.8 (0.01)	39.9 (0.05)	39.2 (0.21)
8	44.3 (0.01)	44.7 (0.01)	45.2 (0.03)	45.2 (0.15)	44.0 (0.22)	43.3 (0.30)	43.1 (0.34)
9	47.6 (0.13)	47.3 (0.16)	46.6 (0.23)	46.6 (0.35)	46.7 (0.44)	47.2 (0.32)	47.3 (0.23)

Discussion

It is indicated that two different difenzoquat species are excited at the two wavelengths, rather than that an inner filter effect gives rise to the spectral changes. In the latter case, the changes would not be confined to the excitation spectrum, but would also be observed in the emission spectrum (Lakowicz, 1983). It had to be established that the observed effects are not due to a fluorescent impurity in difenzoquat. To this end, further extensive purification by cold finger sublimation was carried out, and it was found that the spectral behavior was identical, irrespective of the extent of purification. Moreover, the effects described here are found only with aqueous solutions. In view of this, it has to be concluded that two types of difenzoquat species are present, although the lack of concomitant response in the emission and absorption spectra is unusual. The lack of variation in the emission spectrum also precludes eximer formation as a cause of the observed behavior. The populations of the two species are approximately equal at low difenzoquat concentration, but at higher concentrations there is a significant population shift to the long-wavelength species.

This behavior is indicative of aggregation, which commonly occurs with amphipathic species in aqueous solution (Myers, 1988). Difenzoquat has detergent-like features, combining an ionic extremity with two hydrophobic phenyl groups. Since the latter are relatively compact, the molecule lacks true surfactant behavior such as micelle formation. This was clearly shown by surface tension and conductivity measurements--neither gave the characteristic curves indicative of micellar solutions (Shaw, 1983). However, a degree of aggregation is expected, in which

the hydrophobic portions of two molecules interact, possibly with the ionic headgroups pointing in opposite directions.

The relative population increase of the aggregated species at higher difenzoquat concentration follows the expected behavior and manifests itself through the data shown in Table 3.1. It is notable, however, that the aggregation is not disturbed by an increase in ionic strength or the presence of detergents. SLS micelles, bearing a negative charge, clearly attract positively charged difenzoquat to their surface, giving rise to a great increase in fluorescence intensity. This is probably due to the submersion of the hydrophobic portion of the fluorophore in the hydrocarbon region below the micelle surface, while the ionic part is anchored to the charged interface. This appears to happen equally to difenzoquat monomers and aggregated bodies, without breaking up the latter.

CTAB micelles greatly enhance difenzoquat aggregation, as shown by the considerable increase of the I_1/I_2 ratio. Monomers and premicellar aggregates of the detergent do not have this effect. The large, positively charged CTAB micelle would be expected to repel the difenzoquat cation, but it is possible that the anionic counterion "halo" (Ndou and von Wandruszka, 1988) promotes aggregation of the fluorophore by attracting it into the double-layer.

The relative insensitivity of the difenzoquat emission spectrum to both concentration and detergent effects indicates that both the monomer and the aggregates emit from spectrally similar states. Excitation, on the other hand, is greatly different for the two types of species, with a bathochromic shift of more than 60 nm for the aggregates. The absorption spectrum is shifted hypsochromically by more than 30 nm

relative to the excitation spectrum, indicating the presence of many non-emitting levels in the aggregates. Excitation/absorption dichotomies have been reported for large polycyclic aromatic systems (Fetzer and Schmidt, 1989), but the effects were much smaller than those found here with difenzoquat.

The small energy barrier to simultaneous rotation of the phenyl group in the ground state would allow for a significant population of non-planar molecules at room temperature. However, the larger barrier in the first excited state will ensure that most molecules there are in the planar form. The first excited state is the presumed emission state, and has a large oscillator strength (1.10) in the planar geometry, indicating strong fluorescence.

Comparing the calculated energies and intensities with the observed absorption spectrum, we conclude that in the ground state, the major absorbing species are the non-planar difenzoquat structures. In the calculated spectra, the more planar structures have large intensities at lower energies (29,000 cm^{-1}) and weaker intensities at higher energies (44,000 cm^{-1}). For the larger angles, the lower energy transitions are much weaker and the intensities of the higher energy transitions greatly increase. For the perpendicular structure, we tentatively assign the transitions calculated at 43,100 and 38,300 cm^{-1} to the strong bands observed at 44,000 and 39,000 cm^{-1}. The transition calculated at 39,200 cm^{-1} might contribute to the latter observed band. The experimental absorption spectrum also shows weak features at 25,000 cm^{-1}, and we interpret this as being due to a small fraction of ground state molecules with planar geometry. Our calculations shed no further light on the concentration dependent anomalies in the difenzoquat spectra.

FLUORESCENCE QUENCHING AND POLARIZATION STUDIES OF NAPHTHALENE AND 1-NAPHTHOL INTERACTION WITH HUMIC ACID

M.J. Morra*, M.O. Corapcioglu, R.M.A. von Wandruszka,

D.B. Marshall, and K. Topper

Abstract

Although it is known that the environmental behavior and fate of synthetic organic compounds are altered upon association with humic materials, the nature of this interaction has been a source of controversy. Fluorescence quenching and polarization techniques were used to study interaction between water soluble humic acid and naphthalene and 1-naphthol. Stern-Volmer plots constructed using intensity values for these fluorophores dissolved in humic acid solutions (0 - 25 mg L^{-1}) were linear. The UV/VIS absorption spectra of each fluorophore in the presence and absence of the humic acid quencher were identical. This, in addition to the observed increase in quenching with temperature, indicates a dynamic (collisional) mode of quenching. Fluorescent lifetimes of the probes decreased in the presence of humic acid, providing further evidence of dynamic quenching. However, the slopes of Stern-Volmer plots constructed with lifetime values were considerably smaller than plots obtained with intensity values. Calculated bimolecular quenching constants of 5.2×10^{10} and 4.8×10^{11} $\underline{M}^{-1}$ s^{-1} for naphthalene and 1-naphthol, respectively, are above the maximum considered possible for a diffusion controlled interaction. Fluorescence polarization measurements indicate no rigid association between unquenched 1-naphthol and humic acid. The interaction of naphthalene and 1-naphthol with humic acid in aqueous solution occurs

through a loose association in which humic acid surrounds the fluorophore in a cage-like manner. This pseudo-micelle confines the probe without rigidly binding it, promoting frequent quenching collisions and a combination of dynamic and static quenching.

Introduction

The discrepancies between predicted and observed partition coefficients of synthetic organic compounds with the solid (soil) and liquid (water) phases have usually been ascribed to complexation with water-soluble organics (Gschwend and Wu, 1985; Voice et al., 1983; Voice and Weber, 1985). Interactions between synthetic organic compounds and soluble humic materials isolated from either aquatic or soil systems have been demonstrated (Carter and Suffet, 1982; Madhun et al., 1986; Ballard, 1971; Wijayaratne and Means, 1984; Caron et al., 1985; Tramonti et al., 1986). These interactions may alter the environmental behavior and fate of synthetic organic compounds, including toxicity and bioaccumulation (Dell'Agnola et al., 1981), volatility (Guenzi and Beard, 1974), photolysis (Zepp et al., 1981; Miller et al., 1989), and non-biological alteration (Armstrong and Konrad, 1974; Stevenson, 1976). It has been proposed that water soluble humic materials may act as carriers for pesticides, increasing their transport in the soil profile (Jury et al., 1986; Enfield, 1985). Senesi and Chen (1989) have recently reviewed the mechanisms and consequences of organic chemical interactions with humic materials.

The interaction of nonionic synthetic organic compounds with natural organic materials has been interpreted as both a surface

phenomenon and a partitioning process (Chiou, 1989; Carter and Suffet, 1982; Chiou et al., 1983; Chiou et al., 1986). The lack of a complete understanding of the physicochemical properties of humic materials is partially responsible for this controversy. It has been proposed that humic materials are composed of small molecular weight compounds bound together by a variety of weak bonding mechanisms to form micelles with a hydrophilic exterior and a hydrophobic interior (Wershaw, 1986; Wershaw et al., 1986). Hydrophobic compounds will therefore partition into the interior of humic materials in a manner consistent with the hypothesis of Chiou and co-workers (Chiou et al., 1986).

Fluorescence spectroscopy has been widely used to study both biological and nonbiological micelles (Lakowicz, 1983; Gratzel and Thomas, 1976). However, fluorescence quenching and polarization studies of the interactions of humic materials with synthetic organic compounds have been limited to the determination of equilibrium constants (Gauthier et al., 1986; Traina et al., 1989; Roemelt and Seitz, 1982). In this study we use these techniques to determine the type of association occurring between humic acid and naphthalene and 1-naphthol. The compounds have been identified as degradative products of carbaryl (1-naphthyl methylcarbamate) in soils (Kaufman, 1974) and are potential groundwater pollutants (Zachara et al., 1984). The compounds were chosen instead of more efficient fluorophores, such as pyrene, because of their somewhat greater water solubility. The aqueous solubility of less water soluble compounds is increased upon association with humic materials, either through partitioning into the humic micelle (Chiou et al., 1986) or simply by dispersion of large fluorophore aggregates (Roemelt and Seitz, 1982). Data interpretation would be hindered by the

difficulty of separating fluorophore solubility changes from fluorophore-quencher association.

Theory

Fluorescence quenching is based upon the proportional decrease in fluorescence that occurs with the introduction of a quencher.

$$F_o/F = 1 + k_q \tau_o[Q] = 1 + K[Q]$$

F_o and F are the fluorescence intensities of the fluorophore (synthetic organic compound) in the absence and presence of the quencher (humic acid), respectively, k_q is the bimolecular quenching constant, τ_o is the lifetime of the fluorophore in the absence of the quencher, [Q] is the concentration of the quencher, and $K = k_q \tau_o$ is the Stern-Volmer quenching constant.

A Stern-Volmer plot is constructed using F_o/F as the dependent variable and [Q] as the independent variable. The existence of two types of quenching is recognized, dynamic and static, and when present separately both result in linear Stern-Volmer plots. Dynamic quenching occurs when the excited fluorophore is nonradiatively deactivated during the lifetime of the excited state. The process is collisional in nature and no actual binding occurs between the fluorophore and the quencher. Static quenching is the result of a ground state association between the quencher and fluorophore in which the bound fluorophore no longer fluoresces. In the case of static quenching, K becomes the binding constant, K_s, which is the slope of the Stern-Volmer plot. This

constant is defined as

$$K_S = \frac{[F\text{-}Q]}{[F]\ [Q]}$$

where [F-Q] is the concentration of the complex and [F] is the concentration of the fluorophore. Since both types of quenching result in linear Stern-Volmer plots, additional evidence is required to determine which mechanism is responsible for the observed quenching.

The most definitive evidence for discriminating between static and dynamic quenching is fluorescence lifetime of the fluorophore in the presence (τ) and absence of the quencher. Fluorescence of a compound exhibiting a ground state association will be quenched and lifetime measurements will include only fluorescence of the unbound molecules. The observed lifetime does not change and therefore $\tau_o/\tau = 1$ for static quenching. In contrast, fluorescence lifetime is altered by the dynamic quenching process theoretically resulting in τ_o/τ ratios equivalent to F_o/F. In the case of a combination of static and dynamic quenching, curvature occurs in the Stern-Volmer plot when F_o/F values are used (Lakowicz, 1983).

In those instances in which binding of a fluorophore to a quencher does not result in fluorescence quenching, fluorescence polarization can be used as an alternative technique to determine the extent of interaction. The theory of fluorescence polarization is well established (Weber, 1952; Wahl, 1965; Fayet and Wahl, 1969; Lakowicz, 1983). Fluorescence polarization measurements have been used to assess the adsorption of fluorescent molecules onto larger bodies, such as colloidal clays (von Wandruszka and Brantley, 1979). Fluorescence

polarization has also been used to determine binding constants for perylene and fulvic acids in glycerol solutions (Roemelt and Seitz, 1982).

In fluorescence polarization, polarizers are placed in the excitation and emission beams. Emission intensities are measured with the two polarizers oriented both parallel and perpendicular to each other. The perpendicular intensity component is related to the extent of Brownian motion of the fluorophore in the short time lag between excitation and emission. The larger the fluorescent entity (be it the fluorophore itself, a complex species, or the molecule adsorbed to a larger body), the slower its movement in solution. Slower movement leads to a smaller perpendicularly polarized emission component. This change can therefore be used to monitor the size or attachment of the fluorophore in solution.

The degree of fluorescence polarization is usually expressed in terms of the fluorescence anisotropy, r, which is defined as:

$$r = \frac{I_{\parallel} + I_{\perp}}{I_{\parallel} + 2I_{\perp}}$$

$I_{\parallel}$ is the fluorescence intensity detected through a polarizer with the plane of polarization parallel to the excitation beam and $I_{\perp}$ is the intensity detected through a perpendicularly oriented polarizer.

Materials and Methods

Humic Acid and Reagent Preparation

The top 30 cm of a Latahco silt loam soil (argiaquic Xeric Argialbolls) maintained as pasture for at least 20 yr, was collected, air-dried, and crushed to pass a 20 mm sieve. The collected soil contained 41.5 g organic C, 159 g clay, 121 g silt, and 3.9 g total N kg^{-1} soil. Organic C was determined by the Walkley-Black method (Nelson and Sommers, 1982), particle size distribution by the hydrometer method (Day, 1956), and total N by Dumas combustion (LECO CHN-600 Determinator, St. Joseph, MI). Humic acid extraction was performed in a similar manner as recommended by Schnitzer (1982). Carbonates were removed by HCl acidification and the soil was washed with water prior to humic acid extraction with 0.1 M NaOH. Soil samples were extracted under N_2 for 24 h, soil removed by centrifugation (8400 x g for 10 min), and humic acid precipitated by acidification of the extract to pH 2.0. After 24 h, humic acid was separated from fulvic acid in the extract by centrifugation (880 x g for 30 min). The humic acid precipitate was redissolved in 0.1 M NaOH and the resulting solution was adjusted to pH 7.0. A 50 mL ultrafiltration cell was used in combination with an ultrafiltration membrane (Amicon, Danvers, MA) having a molecular weight cutoff of 10 000 daltons (PM10) to purify the sample. The method used was similar to that reported by Kwak et al. (1977). Deionized water (250-350 mL) contained in a pressurized reservoir (0.345 MPa) was passed through the membrane in a continuous flow mode using N_2. The extract was freeze-dried and stored at room temperature. The resulting freeze-dried humic acid contained, on a moisture free basis, 337 g total C, 26.6 g total N, 34.5 g H, 25.3 g Fe, 30.8 g Al, and 115 g Si kg^{-1} soil.

C, N, and H were determined by Dumas combustion (LECO CHN-600 Determinator, St. Joseph, MI) and Fe, Al, and Si by Inductively Coupled Plasma Emission Spectroscopy (Applied Research Laboratories, Sunland, CA). No attempt was made to further purify the extract.

Fresh humic acid stock solutions (1 g L^{-1}) were prepared weekly in distilled deionized water with the help of ultrasonic agitation. Stock solutions were stored in glass at 4°C. Naphthalene (Bureau of Standards, Washington, DC) and 1-naphthol (Fisher Scientific, Pittsburgh, PA) solutions of 1 x 10^{-4} M were prepared by dissolving the compounds in distilled deionized water with the aid of ultrasonic agitation. Sonication times varied from 2 to 18 h. All stock solutions were stored in the dark at 4°C. Ionic strength of the samples used in fluorescence quenching and polarization measurements was adjusted by addition of the appropriate amount of 0.1 M $NaClO_4$. Humic acid solutions in 1 x 10^{-3} M $NaClO_4$ had an average pH of 6.0.

Fluorescence Quenching

A Perkin-Elmer MPF-66 Fluorescence Spectrophotometer (Norwalk, CT) equipped with a thermostated cell compartment was used for fluorescence measurements. Excitation wavelengths used for naphthalene and 1-naphthol were 275.6 and 291.2 nm, respectively. Emission wavelengths were selected for maximum sensitivity and ranged from 335.6 to 336.6 nm for naphthalene and 466.0 to 470.9 nm for 1-naphthol. Band pass settings for fluorescence quenching were adjusted to 1 nm for both naphthalene and 1-naphthol.

The unquenched fluorescence intensity, F_o, was measured at 25°C in a solution containing 7 x 10^{-5} M of the fluorophore and 1 x 10^{-3} M

$NaClO_4$. An equilibration time of 2 min was allowed after preparation of the solution. Equilibration times of 80 min resulted in no further quenching. Sample solutions used for the measurements of the quenched fluorescence intensity, F, were prepared by addition of various amounts of humic acid to solutions that were otherwise identical to the unquenched solutions. Interference from the humic acid emission was eliminated by instrumental subtraction of the spectrum of a solution containing only humic material from the sample spectrum. Absorbance measurements of humic acid solutions were used to compensate for inner filter effects as described by Gauthier et al. (1986). A Perkin Elmer Lambda 4C UV/VIS spectrophotometer was used for all absorbance measurements. Reported values represent the mean of triplicate measurements.

Sample temperatures were adjusted between 5 and 45°C for 24 mg L^{-1} humic acid solutions to determine changes in fluorescence quenching as a function of temperature. Sample temperature was equilibrated for 10 min.

Fluorescence Lifetimes

The time-resolved fluorescence lifetime curves were obtained using a pulsed laser fluorimeter as described by Wong and Harris (1990). Fluorophore concentrations were 1×10^{-5} M in 0.01 M $NaClO_4$ with quencher (humic acid) concentrations ranging from 0.0 to 125 mg L^{-1}. Oxygen was removed by freeze-pump-thawing the samples. The emission amplitudes of humic acid were sufficiently small such that there were no contributions to the observed decay curves. Decay curves were evaluated by exponential analyses and Stern-Volmer plots were constructed.

Berlman (1971) determined the quantum yields of naphthalene and 1-naphthol in cyclohexane. Using these data, the quantum yields were estimated by comparing fluorescence intensities of the fluorophore in 0.01 M $NaClO_4$ to the fluorophore in cyclohexane.

Fluorescence Polarization

Fluorescence polarization measurements were taken by inserting a pair of matched Glan-Taylor polarizing prisms (Melles Griot, Irvine, CA) in the excitation and emission beams. Excitation and emission wavelengths were selected as noted for fluorescence quenching work and bandpass settings of 8 to 10 nm were used. $I_{\parallel}$ was measured with the excitation and emission polarizers aligned in parallel. Values were obtained for the blank (humic acid only) and sample solutions. $I_{\perp}$ was obtained in a similar way, by aligning the polarizers in a perpendicular position. Corrections were made for the emission of humic acid.

Results and Discussion

Linear Stern-Volmer plots were obtained when 1-naphthol and naphthalene fluorescence was quenched by humic acid (Fig. 4.1). Linearity of a Stern-Volmer plot usually implies that either static or dynamic quenching is taking place, but not both. However, higher quencher concentrations may be necessary in order to reach the point at which deviation from linearity takes place. This topic will be more fully discussed within the context of fluorescent lifetime measurements later in this section. Independent methods must be used to determine if linearity is anticipated at higher concentrations and if so, which quenching mechanism is operative.

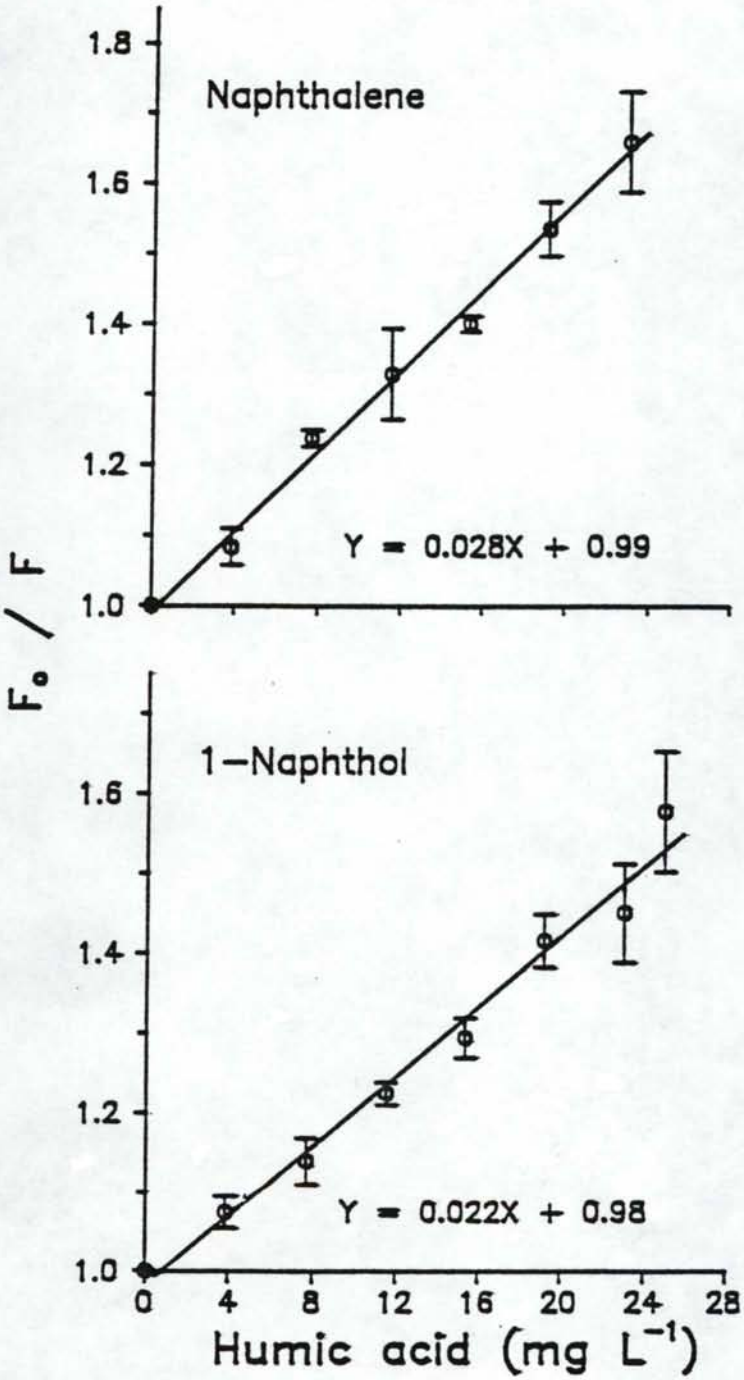

Fig. 4.1. Stern-Volmer plots of naphthalene and 1-naphthol fluorescence quenching by Latahco humic acid. Vertical bars represent one standard deviation.

The first of these methods relies on changes in the UV/VIS absorption spectrum of the fluorophore, which occur when it is involved in a ground state association. Such changes are often observed when the circumstances are equivalent to those in a static fluorescence quenching mechanism. They do not occur in the case of a dynamic quenching interaction, which involves only the excited state of the fluorophore (Lakowicz, 1983). The UV/VIS absorption spectra of the fluorophores in the presence and absence of quencher were essentially identical (data not shown), thus providing no evidence for static quenching.

A second test for discriminating between static and dynamic quenching concerns changes of quenching with temperature. In the case of dynamic quenching, increased temperature is expected to increase the collisional frequency of the fluorophore and quencher, thus increasing quenching and the resulting F_o/F ratio. In contrast, when static quenching occurs, increased temperature is expected to decrease F_o/F ratios as result of dissociation of the fluorophore-quencher complex (Lakowicz, 1983). The value of the F_o/F ratio for 1-naphthol shows a slight positive slope ($P < 0.01$) with increased temperature (Fig. 4.2). Naphthalene quenching also increased with temperature ($P < 0.01$), indicating that dynamic processes may be responsible for the observed quenching (Fig. 4.2).

The most definitive method to discriminate between the two quenching processes is measurement of the fluorescent lifetime of the fluorophore in the presence and absence of quencher. Decreased fluorescent lifetime in the presence of a quencher indicates dynamic quenching, while an unchanged fluorescent lifetime indicates static quenching. The Stern-Volmer plots constructed using τ_o/τ values for 1-

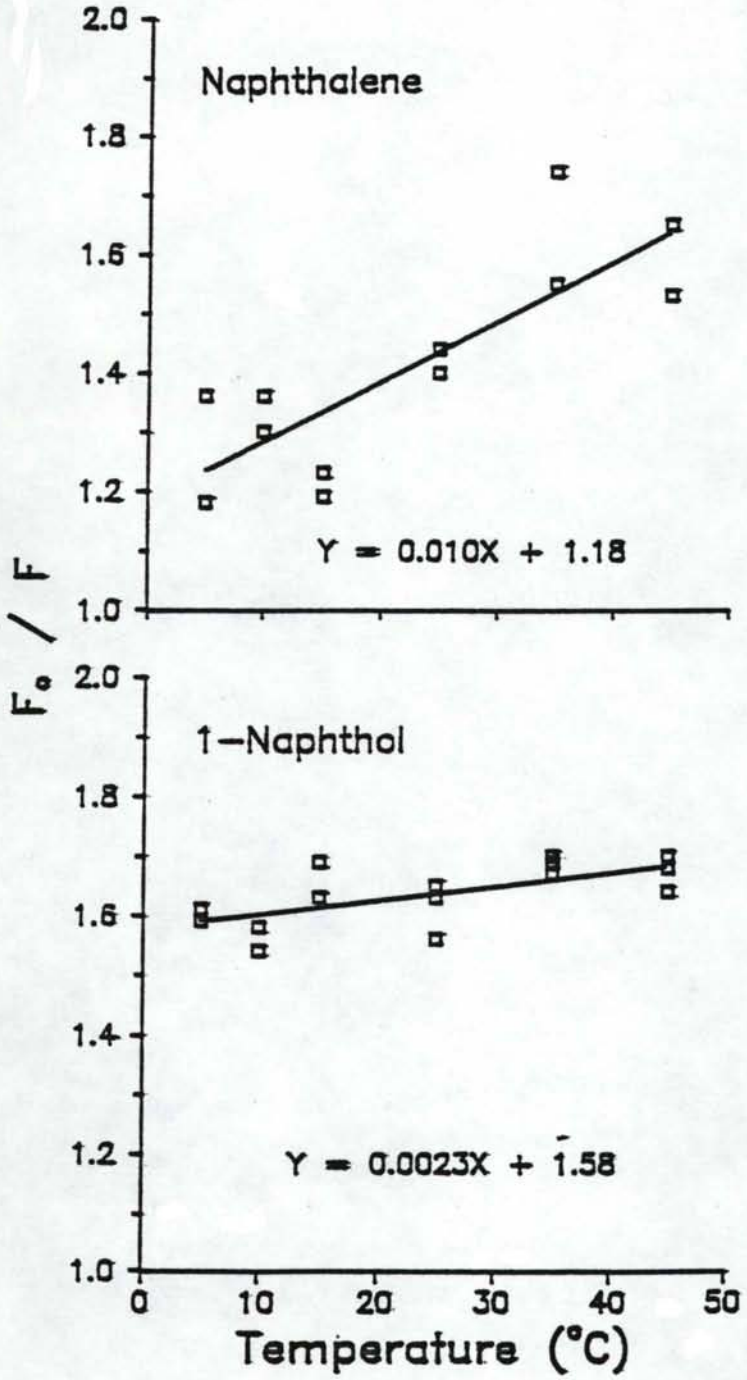

Figure 4.2. Influence of temperature on fluorescence quenching of naphthalene and 1-naphthol by 24 mg L^{-1} Latahco humic acid solutions.

naphthol and naphthalene showed a small positive slope (Table 4.1). This indicates that a collisional mechanism is responsible for the observed quenching of both 1-naphthol and naphthalene fluorescence when in the presence of humic acid.

The slope of the τ_o/τ Stern-Volmer plot is much smaller than the slope of the corresponding F_o/F plot (Fig. 4.1 and Table 4.1). The exact magnitude of this difference depends somewhat on the method used for correction of the inner filter effect (see discussion below). However, under any correction the lifetime slope remains the smaller one. This strongly indicates that a combined mode of quenching is operative: when both static and dynamic quenching occur, a plot of F_o/F vs. quencher concentration over a sufficiently large concentration range will show a positive deviation from linearity (Fig. 4.3). In the present case, the inner filter effect caused by humic acid precludes the use of concentrations higher than 30 mg L^{-1}, and this is probably too low a value to clearly reveal the upward curvature of the plot. On the other hand, the small slope of the lifetime plot relative to the intensity plot is a manifestation of the same phenomenon.

Correction for the inner filter effect produced by humic acid may not be achieved by currently available techniques. Failure to account for absorption of excitation or emission energy by humic acid results in elevated quenching values and a steeper slope for the Stern-Volmer plot. The correction technique used in this work has been applied to humic materials in aqueous solution (Gauthier et al., 1986; Traina et al., 1989), but its accuracy has not been evaluated for such systems. Until the reason for discrepancy between quenching and lifetime Stern-Volmer

Table 4.1. Stern-Volmer analysis of fluorescent lifetime data for 1-naphthol and naphthalene.[a]

Fluorophore	Humic acid	τ_o / τ [b]
	mg L^{-1}	
1-Naphthol	0	1.000 ± 0.0019
	50	1.017 ± 0.0042
	125	1.049 ± 0.0022
	$Y = 0.0004X + 0.999$, $r^2 = 0.98$	
Naphthalene	0	1.000 ± 0.0024
	75	1.011 ± 0.0056
	125	1.021 ± 0.0033
	$Y = 0.0002X + 1.00$, $r^2 = 0.84$	

[a]Reported slopes are significant at $P \leq 0.001$.

[b]Values following ± equal one standard deviation. Mean values for four replicates except for 0 and 125 mg L^{-1} 1-naphthol treatments which are means of five replicates.

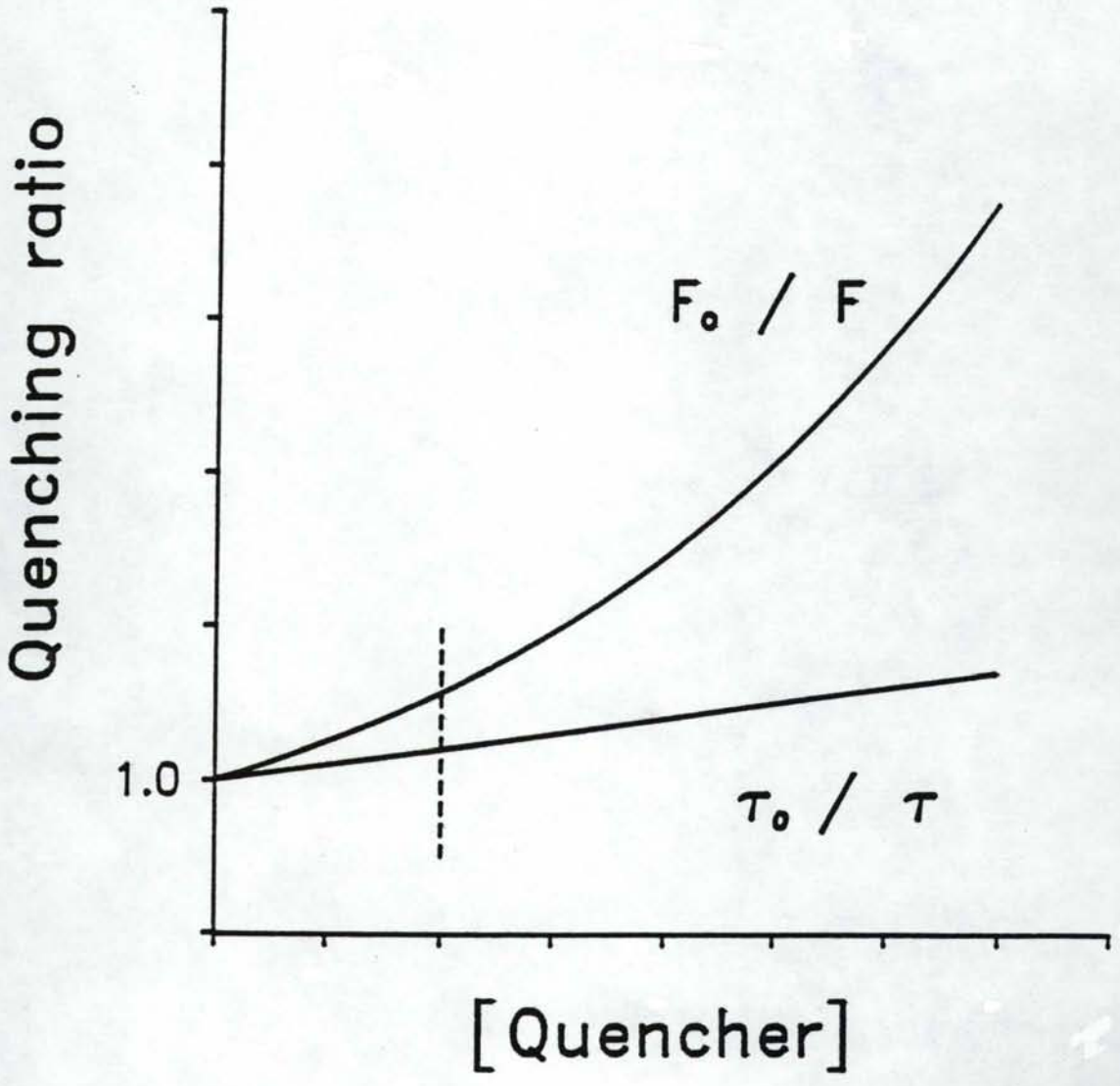

Fig. 4.3. Theoretical Stern-Volmer plots resulting in the case of a combination of static and dynamic quenching (from Lakowicz, 1983). Dotted vertical line represents the maximum humic acid concentration which can be used in the determination of F_o/F ratios.

plots is determined the calculation of equilibrium constants using F_o/F plots must be approached with caution.

Calculation of a bimolecular quenching constant is possible using the relationship between the observed Stern-Volmer quenching constant and the fluorescence lifetime.

$$K = k_q \tau_o$$

The largest value that k_q may assume for a diffusion controlled reaction is approximately 1×10^{10} $\underline{M}^{-1}$ s^{-1} (Lakowicz, 1983). Calculated values for k_q exceeding this value imply that the reaction is too fast to be diffusion controlled and therefore quenching cannot occur as a result of a dynamic mechanism. It is important to note that the solution of this equation has been a source of confusion mainly caused by a lack of careful attention in defining the terms used. The parameter τ_o specifically refers to the fluorescent lifetime in the absence of the quencher, and should not be confused with the intrinsic fluorescent lifetime. These two terms are only equivalent when the fluorescence quantum yield is 1. This was shown not to be the case for both 1-naphthol and naphthalene (Table 4.2). The best treatment of this topic is that of Badley (1976).

Data used in the calculation of lifetime measurements for 1-naphthol and naphthalene in aqueous solution are shown in Table 4.2 along with lifetime values obtained from the literature for organic solvent systems. It is evident that lifetime measurements obtained in organic solvents cannot be used to accurately estimate bimolecular quenching constants for fluorophores in aqueous systems.

Table 4.2. Data used for calculation of naphthalene and 1-naphthol bimolecular quenching constants.

Fluorophore (solvent)	Fluorescent lifetime	Quantum yield
	ns	
1-Naphthol (water)	8.3	0.08
1-Naphthol (cyclohexane)[a]	10.6	0.21
Naphthalene (water)	38.0	0.23
Naphthalene (cyclohexane)[a]	96	0.23

[a]From Berlman (1971).

To obtain the quenching constant, k_q, it is necessary to know the molecular weight of the quencher. It is not possible to obtain an exact molecular weight for humic acid, but average estimates range from 50 000 to 100 000 daltons, with the minimum near 10 000 daltons (Stevenson, 1982). An ultrafiltration membrane with a molecular weight cutoff of 10 000 was used to purify the humic acid used in this study. Assuming a molecular weight of 10 000 daltons provides a relatively conservative estimate of k_q.

Biomolecular quenching constants were calculated using the experimentally determined values for K (Table 4.1) and τ_o (Table 4.2). Assuming a humic acid molecular weight of 10 000 daltons for conversion of K from L mg^{-1} to $\underline{M}^{-1}$ results in k_q values for 1-naphthol and naphthalene of 4.8×10^{11} and 5.2×10^{10} $\underline{M}^{-1}$ s^{-1}, respectively. These values exceed the maximum considered possible for a strictly diffusion controlled reaction and indicate that the fluorophore and quencher must be in close physical association.

Fluorescence polarization measurements indicated no rigid association between unquenched molecules of 1-naphthol and humic acid in aqueous solution (Fig. 4.4). This is significant, since both the fluorescence lifetime and the rotational relaxation time of this fluorophore are expected to be in the range of 10 to 100 ns. Association with the bulky humic acid entity would therefore lead to a significant increase in the fluorescence anisotropy, r, provided that this association is sufficiently strong to curb local movement of the fluorophore. The lack of change in the anisotropy of 1-naphthol upon interaction with humic acid is consistent with the micelle hypothesis which locates the fluorophore in the hydrophobic interior of humic acid

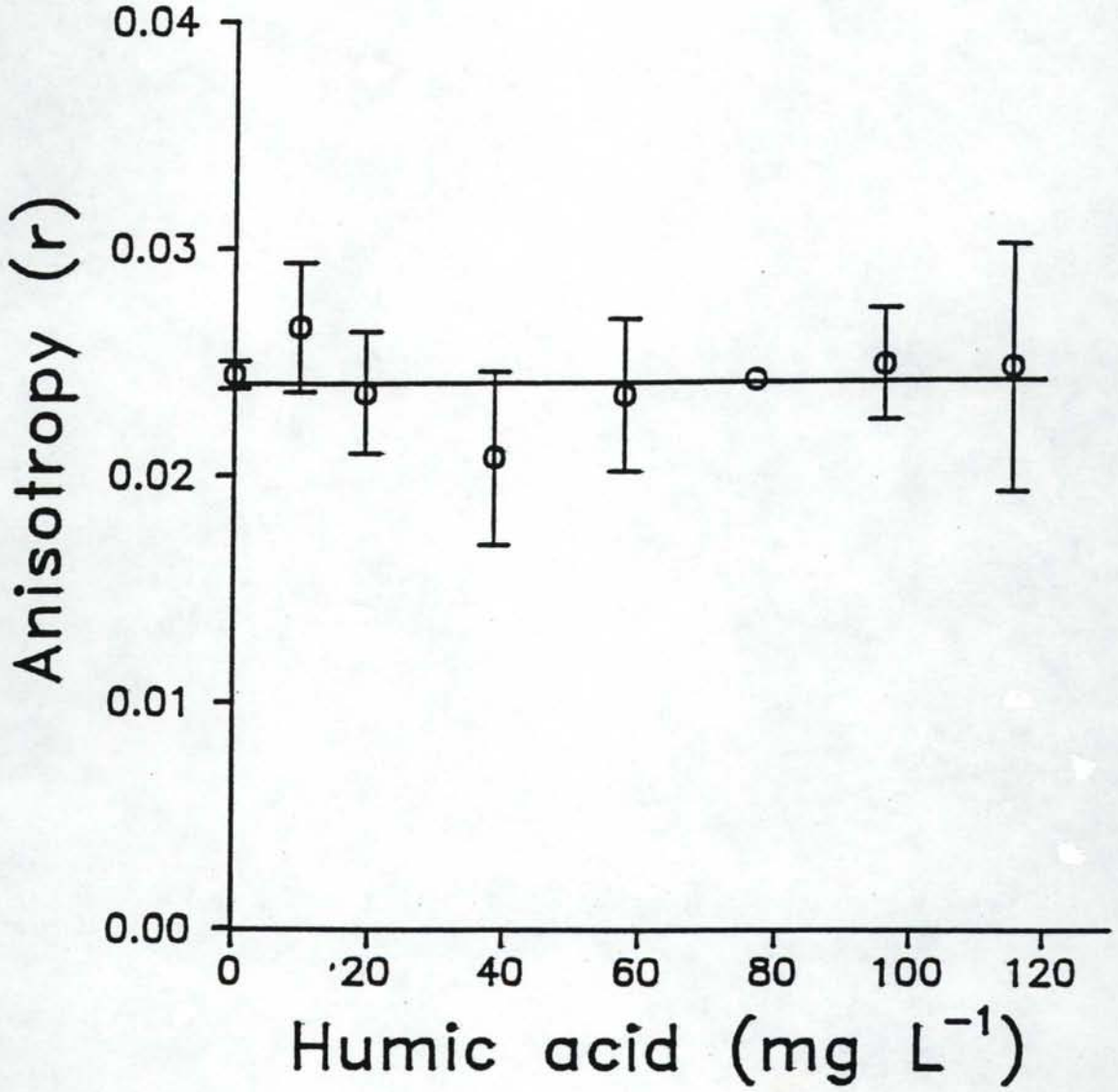

Fig. 4.4. Fluorescence polarization of 1-naphthol and Latahco humic acid in aqueous solution. Vertical bars represent one standard deviation.

(Wershaw, 1986; Wershaw et al., 1986). The fluorophore experiences relatively free local movement in this interior region and the fluorescence anisotropy remains low.

It has been proposed that the critical micelle concentration for humic acid is approximately 10 g L^{-1} (Rochus and Sipos, 1978; Tschapek and Wasowski, 1984; Wershaw et al., 1986). In addition, humic materials are thought to exist as flexible linear polyelectrolytes below 3.5 g L^{-1} and when the solution ionic strength is less than 0.05 M (Schnitzer, 1986). Present experiments were conducted with humic acid concentrations well below these concentrations and a $NaClO_4$ concentration of only 0.001 M. More concentrated humic acid solutions totally quench naphthalene and 1-naphthol fluorescence, making it impossible to use humic acid solutions approaching the concentrations reported above. Although true micelles may not have formed, the combined data indicate a close physical association between the fluorophore and quencher, not unlike a partitioning of the former into a hydrophobic micelle interior (Chiou et al., 1986).

The model proposed here, in which a close proximity between quencher and fluorophore results in an "apparent" static component to the observed quenching is not without precedent (Lakowicz, 1982; Lakowicz and Weber, 1973). Eftink and Ghiron (1976) have reviewed the theories proposed to explain instantaneous deactivation of a fluorophore due to its close proximity to a quencher molecule. In all of these theories, true binding is not a requisite to the quenching process.

The most well known of these theories is the "sphere of action" model which suggests that when the quencher and fluorophore are within a certain maximum distance from each other, apparent static quenching

results. Such a sphere of action that estimates distances specific for individual molecules is provided by the Smoluchowski equation. However, a theory more relevant to the present investigation is the "dark complex" model originally proposed by Boaz and Rollefson (1950) and later applied to micellar systems by Eftink and Ghiron (1976). In this model, quenching occurs without direct physical contact between the fluorophore and quencher. Partitioning of a fluorophore into a micelle interior increases its local concentration, in turn increasing the frequency of collisions with any quenchers that are also present. The apparent static quenching component also increases, because decreased distance between the fluorophore and quencher enhances the quenching process described by the dark complex model (Eftink and Ghiron, 1976). Similarly, the apparent static quenching observed in this study is not caused by true binding, but to a close physical association between the fluorophore and the humic acid entities leading to immediate deactivation of the former.

Conclusions

Both the UV/VIS absorption spectra of naphthalene and 1-naphthol in the presence of humic acid, and the increase of quenching with sample temperature suggest that dynamic fluorescence quenching occurs and that no ground state complex exists between the fluorophores and humic acid. This mode of quenching is also indicated by the decrease in fluorescence lifetime when humic acid is present and by the absence of a measurable increase in fluorescence anisotropy under those conditions. However, bimolecular quenching constants calculated from lifetime measurements

are rather high, suggesting that true dynamic quenching, in which fluorophore and quencher are free and separate in solution, is not operative. Moreover, the much smaller slope of the Stern-Volmer plot derived from τ_o/τ relative to that obtained from F_o/F strongly indicates that dynamic and static quenching occur. These seemingly conflicting findings may be explained by a model that places the fluorophore in close physical proximity to the quencher, without rigidly binding it. Under such circumstances, diffusional quenching need not strictly rely on Brownian motion, and bimolecular quenching constants can indeed exceed those anticipated for a diffusion controlled process. It is proposed that humic acid forms cage-like entities at various points along its constituent chains. These "pockets" resemble micelles, but are larger and looser, probably due to structural constraints inherent in a large convoluted molecule. The interior of the pseudo-micelles is hydrophobic and offers a non-polar environment to the fluorophore. Although the latter has freedom of motion within a relatively roomy cage, it is also close to many quenching centers. Small translational displacements by either humic acid or the fluorophore lead to frequent quenching interactions.

Acknowledgments

The authors wish to thank Dr. J.M. Harris and A.L. Wong at the University of Utah for the use of laser instrumentation necessary in fluorescence lifetime measurements.

REFERENCES

Abrams, S.M., J.S. Shenk, M.O. Westerhaus, and F.E. Barton, II. 1987. Determination of forage quality by near infrared reflectance spectroscopy: efficacy of broad-based calibration equations. J. Dairy Sci. 70:806-813.

Ahmed, M., and J.M. Oades. 1984. Distribution of organic matter and adenosine triphosphate after fractionation of soils by physical procedures. Soil Biol. Biochem. 16:465-470.

Anderson, D.W., S. Saggar, J.R. Bettany, J.W.B. Stewart. 1981. Particle size fractions and their use in studies of soil organic matter: I. The nature and distribution of forms of carbon, nitrogen, and sulfur. Soil Sci. Soc. Am. J. 45:767-772.

Anderson, R.L., and L.A. Nelson. 1975. A family of models involving intersecting straight lines and concomitant experimental designs useful in evaluating response to fertilizer nutrients. Biometrics 31:303-318.

Armstrong, D.E. and J.G. Konrad. 1974. Nonbiological degradation of pesticides. p. 123-131. In W.D. Guenzi (ed.) Pesticides in soil and water. SSSA, Madison, WI.

Bacon, A.D., and M.C. Zerner. 1979. An intermediate neglect of differential overlap theory for transition metal complexes: iron, cobalt and copper chlorides. Theor. Chim. Acta 53:21-54.

Badley, R.A. 1976. Fluorescent probing of biological membranes. p. 91-168. In E.L. Wehry (ed.) Modern fluorescence spectroscopy, Vol. 2. Plenum Press, New York.

Ballard, T.M. 1971. Role of humic carrier substances in DDT movement through forest soil. Soil Sci. Soc. Amer. Proc. 35:145-147.

Berlman, I.S. 1971. Handbook of fluorescence spectra of aromatic molecules, 2nd ed. Academic Press, New York.

Boaz, H. and G.K. Rollefson. 1950. The quenching of fluorescence. Deviations from the Stern-Volmer law. J. Am. Chem Soc. 72:3435-3443.

Bowen, J.M., S.V. Compton, and M.S. Blanche. 1989. Comparison of sample preparation methods for the Fourier Transform Infrared analysis of an organo-mineral sorption mechanism. Anal. Chem. 61:2047-2050.

Bowers, S.A., and R.J. Hanks. 1965. Reflection of radiant energy from soils. Soil Sci. 100:130-138.

Bowman, R.S. and R.C. Rice. 1986. Transport of conservative tracers in the field under intermittent flood irrigation. Water Resour. Res. 22: 1531-1536.

Bruck, G.R. 1986. Pesticide and nitrate contamination of ground water near Ontario, Oregon. U.S. Environmental Protection Agency, Seattle, WA.

Bruckert, S. 1982. Analysis of the organo-mineral complexes of soils. In Constituents and properties of soils. M. Bonneau and B. Souchier (eds.). Academic Press, London, pp. 214-237.

Caron, G., I.H. Suffet, T. Belton. 1985. Effect of dissolved organic carbon on the environmental distribution of nonpolar organic compounds. Chemosphere 8:993-1000.

Carter, C.W. and I.H. Suffet. 1982. Binding of DDT to dissolved humic materials. Environ. Sci. Technol. 16:735-740.

Chichester, F.W. 1969. Nitrogen in soil organo-mineral sedimentation fractions. Soil Sci. 107:356-363.

Chiou, C.T. 1989. Theoretical considerations of the partition uptake of nonionic organic compounds by soil organic matter. p. 1-29. In B.L. Sawhney and K. Brown (ed.) Reactions and movement of organic chemicals in soils. SSSA Spec. Publ. 22. SSSA and ASA, Madison, WI.

Chiou, C.T., P.E. Porter, and D.W. Schmedding. 1983. Partition equilibria of nonionic organic compounds between soil organic matter and water. Environ. Sci. Technol. 17:227-231.

Chiou, C.T., P.E. Porter, and D.W. Schmedding. 1983. Partition equilibria of nonionic organic compounds between soil organic matter and water. Environ. Sci. Technol. 17:227-231.

Chiou, C.T., R.L. Malcolm, T.I. Brinton, and D.E. Kile. 1986. Water solubility enhancement of some organic pollutants and pesticides by dissolved humic and fulvic acids. Environ. Sci. Technol. 20:502-508.

Christensen, B.T. 1985. Carbon and nitrogen in particle size fractions isolated from Danish soils by ultrasonic dispersion and gravity-sedimentation. Acta Agric. Scand. 35:175-187.

Christensen, B.T. 1987. Decomposability of organic matter in particle size fractions from field soils with straw incorporation. Soil Biol. Biochem. 19:429-435.

Clark, D.H., E.E. Cary, and H.F. Mayland. 1989. Analysis of trace elements in forages by near infrared reflectance spectroscopy. Agron. J. 81:91-95.

Clark, D.H., H.F. Mayland, and R.C. Lamb. 1987. Mineral analysis of forages with near infrared reflectance spectroscopy. Agron. J. 79:485-490.

Dalal, R.C., and R.J. Henry. 1986. Simultaneous determination of moisture, organic carbon, and total nitrogen by near infrared reflectance spectrophotometry. Soil Sci. Soc. Am. J. 50:120-123.

Day, P.R. 1956. Report of the committees on physical analyses, 1954-55. Soil Sci. Soc. Am. Proc. 20:167-169.

Dell'Agnola, G., G. Ferrari, and S. Nardi. 1981. Antidote action of humic substances on atrazine inhibition of sulfate uptake in barley roots. Pestic. Biochem. Physiol. 15:101-104.

Edwards, W.D., and M.C. Zerner. 1983. Electronic structure of model chlorophyll systems. Int. J. Quantum Chem. 23:1407-1432.

Eftink, M.R. and C.A. Ghiron. 1976. Fluorescence quenching of indole and model micelle systems. J. Phys. Chem. 80:486-493.

Enfield, C.G. 1985. Chemical transport facilitated by multiphase flow systems. Water Sci. Technol. 17:1-12.

Enfield, C.G. and G. Bengtsson. 1986. Hexachlorobenzene transport facilitated by macromolecules. Agronomy Abstracts, p. 156. Annual Meetings American Society of Agronomy, New Orleans, LA.

Enfield, C.G., G. Bengtsson, and R. Lindqvist. 1989. Influence of macromolecules on chemical transport. Environ. Sci. Technol. 23:1278-1286.

Escudey, M., M. de la Luz Mora, P. Diaz, and G. Galindo. 1989. Apparent dissolution during ultrasonic dispersion of allophanic soils and soil fractions. Clays Clay Miner. 37:493-496.

Everts, C.J., R.S. Kanwar, E.C. Alexander, Jr., and S.C. Alexander. 1989. Comparison of tracer mobilities under laboratory and field conditions. J. Environ. Qual. 18:491-498.

Fayet, M. and Ph. Wahl. 1969. Etude du declin de la fluorescence polarisee de la q-globuline de lapin conjugee avec l'isothiocyanate de fluoresceine. Biochim. Biophys. Acta 181:373-380.

Fetzer, J.C., and W. Schmidt. 1989. The electronic spectrometry of two similar tetrabenzoperylene isomers. Spectrochim. Acta 45A:503-505.

Gauthier, T.D., E.C. Shane, W.F. Guerin, W.R. Seitz, and C.L. Grant. 1986. Fluorescence quenching method for determining equilibrium constants for polycyclic aromatic hydrocarbons binding to dissolved humic materials. Environ. Sci. Technol. 20:1162-1166.

Genrich, D.A. and J.M. Bremner. 1972. A reevaluation of the ultrasonic-vibration method of dispersing soils. Soil Sci. Soc. Amer. Proc. 36:944-947.

Genrich, D.A. and J.M. Bremner. 1974. Isolation of soil particle-size fractions. Soil Sci. Soc. Amer. Proc. 38:222-225.

Gratzel, M. and J.K. Thomas. 1976. The application of fluorescence techniques to the study of micellar systems. p. 169-216. In E.L. Wehry (ed.) Modern fluorescence spectroscopy, Vol. 2. Plenum Press, New York.

Gregorich, E.G., R.G. Kachanoski, and R.P. Voroney. 1988. Ultrasonic dispersion of aggregates: Distribution of organic matter in size fractions. Can. J. Soil Sci. 68:395-403.

Gregorich, E.G., R.G. Kachanoski, and R.P. Voroney. 1989. Carbon mineralization in soil size fractions after various amounts of aggregate disruption. J. Soil Sci. 40:649-659.

Gschwend, P.M. and S. Wu. 1985. On the constancy of sediment-water partition coefficients of hydrophobic organic pollutants. Environ. Sci. Technol. 19:90-96.

Guenzi, W.D. and W.E. Beard. 1974. Volatilization of pesticides. p. 107-122. In W.D. Guenzi (ed.) Pesticides in soil and water. SSSA, Madison, WI.

Hall, M.H., S.M. Dutro, and M.J. Klowden. 1990. Near infrared reflectance spectroscopy determination of mosquito (Diptera: Cluicidae) blood meal size. J. Med. Entom. 27:76-79.

Hamblin, A.P. 1977. Structural features of aggregates in some east Anglian silt soils. J. Soil Sci. 28:23-28.

Hayes, M.H.B. 1986. Nature and properties of humus-mineral complexes. In Interactions of soil minerals with natural organics and microbes, SSSA Spec. Publ. 17. P.M. Huang and M. Schnitzer (eds.). Soil Sci. Soc. Am., Madison, Wis., pp. 103-158.

Head, J.D., and M.C. Zerner. 1985. A Broyden-Fletcher-Goldfarb-Shannon optimization procedure for molecular geometries. Chem. Phys. Lett. 122:264-270.

Herbicide Handbook, 5th ed. 1983. Weed Science Society of America, Champaign, IL.

Hinds, A.A. and L.E. Lowe. 1980a. Dispersion and dissolution effects during ultrasonic dispersion of gleysolic soils in water and in electrolytes. Can. J. Soil Sci. 60:329-335.

Hinds, A.A. and L.E. Lowe. 1980b. The use of an ultrasonic probe in soil dispersion and in the bulk isolation of organo-mineral complexes. Can J. Soil Sci. 60:389-392.

Huling, S.G. 1989. Facilitated transport. EPA, Center for Environmental Research, Cincinnati, OH. EPA/540/4-89/003.

Huling, S.G. 1989. Superfund ground water issue-facilitated transport. EPA/540/4-89/003. U.S. Environmental Protection Agency, Center for Environmental Research Information, Cincinnati, Oh.

Hunter, C.R. and A.J. Busacca. 1989. Dispersion of three andic soils by ultrasonic vibration. Soil Sci. Soc. Am. J. 53:1299-1302.

Iwaoka, T., S.-H. Wang, and P.R. Griffiths. 1985. Diffuse reflectance infrared spectrometry of inorganic materials. Spectrochim. Acta. 41A:37-41.

Jackson, M.L. 1956. Soil chemical analysis-advanced course. University of Wisconsin, Madison, WI.

Jury, W.A. and M. Ghodrati. 1987. Overview of organic chemical environmental fate and transport modeling approaches. Agronomy Abstracts, p. 274. Annual Meetings, American Society of Agronomy, Atlanta, GA.

Jury, W.A., H. Elabd, and M. Resketo. 1986. Field study of napropamide movement through unsaturated soil. Water Resour. Res. 22:749-755.

Kaufman, D.D. 1974. Degradation of pesticides by soil microorganisms. p. 133-202. In W.D. Guenzi (ed.) Pesticides in soil and water. SSSA, Madison, WI.

Krishnan, P., J.D. Alexander, B.J. Butler, and J.W. Hummel. 1980. Reflectance technique for predicting soil organic matter. Soil Sci. Soc. Am. J. 44:1282-1285.

Kwak, J.C.T., R.W.P. Nelson, and D.S. Gamble. 1977. Ultrafiltration of fulvic and humic acids, a comparison of stirred cell and hollow fiber techniques. Geochim. Cosmochim. Acta 41:993-996.

Lakowicz, J.R. 1983. Principles of fluorescence spectroscopy. Plenum Press, New York.

Lakowicz, J.R. and G. Weber. 1973. Quenching of fluorescence by oxygen. A probe for structural fluctuations in macromolecules. Biochemistry 12:4161-4170.

Lee, D.-Y. and W.J. Farmer. 1989. Dissolved organic matter interaction with napropamide and four other nonionic pesticides. J. Environ. Qual. 18:468-474.

MacCarthy, P. and H.B. Mark, Jr. 1975. Infrared studies on humic acid in deuterium oxide: I. Evaluation and potentialities of the technique. Soil Sci. Soc. Amer. Proc. 39:663-668.

MacCarthy, P. and J.A. Rice. 1985. Spectroscopic methods (other than NMR) for determining functionality in humic substances. p. 527-559. In G.R. Aiken et al. (ed.) Humic substances in soil, sediment, and water. John Wiley & Sons, New York.

MacCarthy, P., H.B. Mark, Jr., P.R. Griffiths. 1975. Direct measurement of the infrared spectra of humic substances in water by fourier transform infrared spectroscopy. J. Agric. Food Chem. 23:600-602.

MacIntyre, W.G. and T.B. Stauffer. 1988. Liquid chromatography application to determination of sorption on aquifer materials. Chemosphere 17:2161-2173.

Madhun, Y.A., J.L. Young, and V.H. Freed. 1986. Binding of herbicides by water-soluble organic materials from soil. J. Environ. Qual. 15:64-68.

Marten, G.C., G.E. Brink, D.R. Buxton, J.L. Halgerson, and J.S. Hornstein. 1984. Near infrared reflectance spectroscopy analysis of forage quality in four legume species. Crop Sci. 24:1179-1182.

Marten, G.C., J.L. Halgerson, and J.H. Cherney. 1983. Quality prediction of small grain forages by near infrared reflectance spectroscopy. Crop Sci. 23:94-96.

Marten, G.C., J.S. Shenk, and F.E. Barton, II (ed.). 1989. Near infrared reflectance spectroscopy (NIRS): analysis of forage quality. ARS Agric. Handb. 643, U.S. Gov. Print. Office, Washington, DC.

McCarthy, J.F., and J.M. Zachara. 1989. Subsurface transport of contaminants. Environ. Sci. Technol. 23:496-502.

Miller, G.C., V.R. Hebert, and W.W. Miller. 1989. Effect of sunlight on organic contaminants at the atmosphere-soil interface. p. 99-110. In B.L. Sawhney and K. Brown (ed.) Reactions and movement of organic chemicals in soils. SSSA Spec. Publ. 22. SSSA and ASA, Madison, WI.

Morra, M.J., D.B. Marshall, and C.M. Lee. 1989. FT-IR analysis of humic acid in water using cylindrical internal reflectance. Commun. Soil Sci. Plant Anal. 20:851-867.

Mortland, M.M. 1986. Mechanisms of adsorption of nonhumic organic species by clays. In Interactions of soil minerals with natural organics and microbes, SSSA Spec. Publ. 17. P.M. Huang and M. Schnitzer (eds.). Soil Sci. Soc. Am., Madison, Wis., pp. 59-76.

Myers, D. 1988. Surfactant science and technology. VCH, New York.

Ndou, T.T., and R. von Wandruszka. 1988. Quenching of pyrene fluorescence in premicellar solutions. Anal. Lett. 21:2091-2105.

Nelson, D.W. and L.E. Sommers. 1982. Total carbon, organic carbon, and organic matter. p. 539-579. In A.L. Page et al. (ed.) Methods of soil analysis. Part 2. 2nd ed. Agronomy Monogr. 9. ASA and SSSA, Madison, WI.

North, P.F. 1976. Towards an absolute measurement of soil structural stability using ultrasound. J. Soil Sci. 27:451-459.

Pople, J.A., D.L. Beveridge, and P.A. Dobosh. 1976. Approximate self-consistent molecular-orbital theory. V. intermediate neglect of differential overlap. J. Chem. Phys. 47:2026-2033.

Ridley, J.E., and M.C. Zerner. 1973. Intermediate neglect of differential overlap (INDO) technique for spectroscopy. Pyrrole and azines. Theor. Chim. Acta 32:111-134.

Ridley, J.E., and M.C. Zerner. 1976. Triplet states via intermediate neglect of differential overlap: benzene, pyridine and the diazines. Theor. Chim. Acta 42:223-236.

Rochus, W. and S. Sipos. 1978. Die micellbildung bei huminstoffen. Agrochimica 22:446-454.

Roemelt, P.M. and W.R. Seitz. 1982. Fluorescence polarization studies of perylene-fulvic acid binding. Environ. Sci. Technol. 16:613-616.

Schnitzer, M. 1982. Organic matter characterization. In A.L. Page et al. (ed.) Methods of soil analysis. Part 2. 2nd ed. Agronomy 9:581-594.

Schnitzer, M. 1982. Organic matter characterization. p. 581-594. In A.L. Page et al. (ed.) Methods of soil analysis. Part 2. 2nd ed. Agronomy Monogr. 9. ASA and SSSA, Madison, WI.

Schnitzer, M. 1986. Binding of humic substances by soil mineral colloids. p. 77-101. In P.M. Huang and M. Schnitzer (ed.) Interactions of soil minerals with natural organics and microbes. SSSA Spec. Publ. 17. SSSA, Madison, WI.

Schnitzer, M. and S.U. Khan. 1972. Humic substances in the environment. Marcel Dekker, New York.

Schwarzenbach R.P. and J. Westall. 1981. Transport of nonpolar organic compounds from surface water to groundwater. Laboratory sorption studies. Environ. Sci. Technol. 15:1360-1367.

Scotter, D.R. 1978. Preferential solute movement through larger soil voids. I. Some computations using simple theory. Aust. J. Soil Res. 16:257-267.

Senesi, N. and C. Testini. 1982. Physico-chemical investigations of interaction mechanisms between s-triazine herbicides and soil humic acids. Geoderma 28: 129-146.

Senesi, N. and Y. Chen. 1989. Interactions of toxic organic chemicals with humic substances. p. 37-90. In Z. Gerstl et al. (ed.) Toxic organic chemicals in porous media. Springer-Verlag, Berlin.

Shaw, D.J. 1983. Introduction to colloid and surface chemistry. Butterworths, London.

Shenk, J.S., I. Landa, M.R. Hoover, and M.O. Westerhaus. 1981. Description and evaluation of near infrared reflectance spectro-computer for forage and grain analysis. Crop Sci. 21:355-358.

Spycher, G. and J.L. Young. 1977. Density fractionation of water-dispersible soil organic-mineral particles. Commun. Soil Sci. Plant Anal. 8:37-48.

Steel, R.G.D., and J.H. Torrie. 1980. Principles and procedures of statistics, 2nd ed. McGraw-Hill, New York.

Stevenson, F.J. 1976. Organic matter reactions involving pesticides in soil. p. 180-207. In D.D. Kaufman et al. (ed.) Bound and conjugated pesticide residues. ACS Symposium Series 29. ACS, Washington, DC.

Stevenson, F.J. 1982. Humus chemistry. John Wiley & Sons, New York.

Sullivan, J.D. and G.T. Felbeck, Jr. 1968. A study of the interaction of s-triazine herbicides with humic acids from three different soils. Soil Sci. 106:42-52.

Theng, B.K.G. 1974. The chemistry of clay-organic reactions. John Wiley & Sons, New York.

Theng, B.K.G. 1979. Formation and properties of clay-polymer complexes. Elsevier, Amsterdam.

Traina, S.J., D.A. Spontak, and T.J. Logan. 1989. Effects of cations on complexation of naphthalene by water soluble organic carbon. J. Environ. Qual. 18:221-227.

Tramonti, V., R.H. Zienius, and D.S. Gamble. 1986. Solution phase interaction of lindane with fulvic acid: Effect of solution pH and ionic strength. Int. J. Environ. Anal. Chem. 24:203-212.

Tschapek, M. and C. Wasowski. 1984. Humic acid: its adsorption at the water/benzene interface. Agrochimica 28:1-8.

van der Marel, H.W. and H. Beutelspacher. 1976. Atlas of infrared spectroscopy of clay minerals and their admixtures. Elsevier, Amsterdam.

van Genuchten, M. Th. 1981. Non-equilibrium transport parameters from miscible displacement experiments. Research Report No. 119. U.S. Salinity Laboratory, USDA-SEA-AR, Riverside, California.

van Genuchten, M.Th. and R.J. Wagenet. 1989. Two-site/two-region models for pesticide transport and degradation: Theoretical Development and Analytical Solutions. Soil Sci. Soc. Am. J. 53:1303-1310.

Voice, T.C. and W.J. Weber, Jr. 1985. Sorbent concentration effects in liquid/solid partitioning. Environ. Sci. Technol. 19:789-796.

Voice, T.C., C.P. Rice, and W.J. Weber, Jr. 1983. Effect of solids concentration on the sorptive partitioning of hydrophobic pollutants in aquatic systems. Environ. Sci. Technol. 17:513-518.

Voice, T.C., C.P. Rice, and W.J. Weber, Jr. 1983. Effect of solids concentration on the sorptive partitioning of hydrophobic pollutants in aquatic systems. Environ. Sci. Technol. 17:513-518.

von Wandruszka, R. and S. Brantley. 1979. A fluorescence polarization study of polyaromatic hydrocarbons adsorbed on colloidal kaolin. Anal. Lett. 12:1111-1122.

Wahl, M.P. 1965. Sur l'etude des solutions de macromolecule par la decroissance de la fluorescence polarisee. C.R. Hebd. Seances Acad. Sci. Paris, 260:6891-6893.

Watson, J.R. 1971. Ultrasonic vibration as a method of soil dispersion. Soils Fertil. 34:127-134.

Watson, J.R. and J.W. Parsons. 1974. Studies of soil organo-mineral fractions, I. Isolation by ultrasonic dispersion. J. Soil Sci. 25:1-8.

Weast, R.C. 1975. Handbook of chemistry and physics, 56th ed. CRC Press, Cleveland, Oh.

Weber, G. 1952. Polarization of the fluorescence of macromolecules, 1. Theory and experimental method. Biochem. J. 51:145-155.

Wershaw, R.L. 1985. Application of nuclear magnetic resonance spectroscopy for determining functionality in humic substances. p. 561-584. In G.R. Aiken et al. (ed.) Humic substances in soil, sediment, and water. John Wiley & Sons, New York.

Wershaw, R.L. 1986. A new model for humic materials and their interactions with hydrophobic organic chemicals in soil-water or sediment-water systems. J. Contam. Hydrol. 1:29-45.

Wershaw, R.L., K.A. Thorn, D.J. Pinckney, P. MacCarthy, J.A. Rice, and H.F. Hemond. 1986. Application of a membrane model to the secondary structure of humic materials in peat. p. 133-157. In C.H. Fuchsman (ed.) Peat and Water. Elsevier, Amsterdam.

Westerhaus, M.O. 1989a. Equation development. p. 38-39. In G.C. Marten et al. (ed.) Near infrared reflectance spectroscopy (NIRS): analysis of forage quality. ARS Agric. Handb. 643, U.S. Gov. Print. Office, Washington, DC.

Westerhaus, M.O. 1989b. Validation. p. 40. In G.C. Marten et al. (ed.) Near infrared reflectance spectroscopy (NIRS): analysis of forage quality. ARS Agric. Handb. 643, U.S. Gov. Print. Office, Washington, DC.

Wetzel, D.L. 1983. Near-infrared reflectance analysis: sleeper among spectroscopic techniques. Anal. Chem. 55:1165A-1176A.

Wijayaratne, R.D. and J.C. Means. 1984. Affinity of hydrophobic pollutants for natural estuarine colloids in aquatic environments. Environ. Sci. Technol. 18:121-123.

Wilson, M.A. 1984. Soil organic matter maps by nuclear magnetic resonance. J. Soil Sci. 35:209-215.

Wilson, M.A. 1985. Whole soil NMR applications to soil productivity and classification. Agronomy Abstracts, p. 163. Annual Meetings, American Society of Agronomy, Chicago, IL.

Windham, W.R., D.R. Mertens, and F.E. Barton, II. 1989. 1. Protocol for NIRS Calibration: Sample selection and equation development and validation. p. 96-103. In G.C. Marten et al. (ed.) Near infrared reflectance spectroscopy (NIRS): analysis of forage quality. ARS Agric. Handb. 643, U.S. Gov. Print. Office, Washington, DC.

Windham, W.R., F.E. Barton, II, and J.A. Robertson. 1988. Moisture analysis of forage by near infrared reflectance spectroscopy: preliminary collaborative study and comparison between Karl Fischer and oven drying reference methods. J. Assoc. Off. Anal. Chem. 71:256-262.

Wong, A.L. and J.M. Harris. 1990. Quantitative estimation of component amplitudes in multiexponential data: Application to time-resolved fluorescence spectroscopy. Anal. Chem. (in press).

Zachara, J.M., L.J. Felice, R.G. Riley, F.L. Harrison, B. Mallon, and F.J. Wobber. 1984. The selection of organic chemicals for subsurface transport research. DOE/ER-0217. U.S. Department of Energy, Washington, DC.

Zepp, R.G., G.L. Baughman, and P.F. Schlotzhauer. 1981. Comparison of photochemical behavior of various humic substances in water: I. Sunlight induced reactions of aquatic pollutants photosensitized by humic substances. Chemosphere 10:109-117.

Zerner, M.C., G.H. Loew, and Z.S. Herman. 1980. Calculated optical spectrum of model oxyheme complex. Int. J. Quantum Chem. 18:481-492.

Zielke, R.C., T.J. Pinnavaia, and M.M. Mortland. 1989. Adsorption and reactions of selected organic molecules on clay mineral surfaces. In Reactions and movement of organic chemicals in soils, SSSA Spec. Publ. 22. B.L. Sawhney and K. Brown (eds.). Soil Sci. Soc. Am., Madison, Wis., pp. 81-97.

APPENDIX A

COMMUN. IN SOIL SCI. PLANT ANAL., 20(7&8), 851-867 (1989)

FT-IR ANALYSIS OF ALDRICH HUMIC ACID IN WATER USING CYLINDRICAL INTERNAL REFLECTANCE[1]

M.J. Morra, D.B. Marshall[2], and C.M. Lee[3]

Division of Soil Science
University of Idaho
Moscow, Idaho 83843

ABSTRACT

Recent development of the Cylindrical Internal Reflectance (CIR) sample cell has made infrared analysis of solutes in highly infrared-absorbing solvents such as water possible. Fourier Transform Infrared spectroscopy (FT-IR) has been combined with a CIR sample cell to determine the spectra of Aldrich humic acid in water at concentrations as low as 0.5 g L^{-1}. Spectral scans from 670 to 4000 cm^{-1} indicate that the region of greatest resolution for observing characteristic humic acid absorbance bands occurs from 1000 to 2000 cm^{-1}. Comparison of CIR spectra with Nujol mull and KBr spectra demonstrated a near total elimination of absorbance peaks from 1000 to 1200 cm^{-1} in the nonaqueous preparations. Solution phase parameters were altered to illustrate that the spectra of Aldrich humic acid in water varied with humic acid concentration, ionic strength, and pH. The

[1]Salaries and research support were provided by the Idaho Water Resources Research Institute (Grant No. G1419-32) and by State and Federal funds appropriated to the University of Idaho.
[2]Dept. of Chemistry and Biochemistry, Utah State Univ., Logan, UT 84322.
[3]Dept. of Chemistry, Univ. of Idaho, Moscow, ID 83843.

ability to determine infrared spectra of humic materials in their native wet state will prove advantageous in determining humic material interaction with inorganic and organic pollutants such as trace elements and pesticides.

INTRODUCTION

Humic and fulvic acids have been operationally defined as NaOH extractable soil organic fractions insoluble and soluble in acid, respectively. The fractions therefore necessarily represent heterogeneous mixtures of organic materials possessing a range in chemical characteristics. Previous studies involving infrared analyses of humic or water soluble soil materials have been conducted with dried material pressed into KBr disks (1,2,3), Nujol mulls (4,5), or solid films (6,7). Such drastic procedures may not only alter the extracted materials (8,9), but do not allow for spectral observation of the materials in their native wet state. Analysis in the presence of water has been conducted, but in both reported instances a humic acid slurry was used rather than an aqueous solution (10,11). The lack of infrared studies using aqueous solutions of humic materials has occurred because of the formidable problems associated with measuring infrared solution spectra in a highly infrared-absorbing solvent such as water.

The use of cylindrical internal reflectance (CIR) in Fourier Transform Infrared spectroscopy (FT-IR) represents a recently developed approach to obtain the infrared spectra of dissolved materials in aqueous solution. The theory and practical applications of CIR have previously been described (12), but will be summarized here because no studies with soil extracts have been reported in the literature.

Infrared radiation passes through a rod-shaped crystal possessing a high refractive index and cone-shaped ends (Fig. 1). The cone-shaped ends cause input infrared radiation to be directed

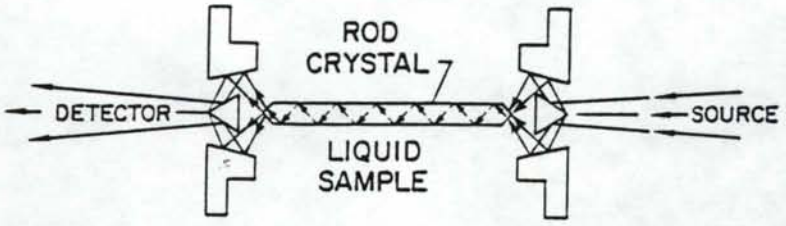

FIGURE 1. Optical Configuration of the Cylindrical Internal Reflectance Sample Cell.

at the angle of incidence necessary for reflection off crystal walls and transmission to the output end of the crystal. Infrared radiation penetrates the liquid surrounding the rod-shaped crystal to a fixed distance sufficiently small so as to prevent highly infrared-absorbing solvents from obscuring spectral observation of contained solutes. When working with aqueous solutions, computer subtraction can be used to eliminate water absorbance bands from the spectra of water plus dissolved material. This technique has been used for both qualitative and quantitative analysis of biological and nonbiological liquids (13,14). CIR has also been successfully applied to studies of the geothite-aqueous solution interface (15).

Commercially available Aldrich humic acid is used to demonstrate the advantages and limitations of CIR for the infrared analysis of natural organic materials. This material was chosen because relatively large quantities (500 g) of a single humic material were required. The Na^+ form was used because it is freely soluble in aqueous solution. The distinction between commercially available humic acid and actual soil extracts is fully appreciated (16). However, the focus here is not on the definitive assignment of absorbance bands to distinct functional groups, but rather on the utility of the aqueous sample technique as compared to nonaqueous preparation techniques in the infrared analysis of natural organic materials.

MATERIALS AND METHODS

A Digilab FTS-80 FT-IR spectrometer with a computer data system, MCT detector, 0.25 cm^{-1} resolution, and a spectral range of 5000 to 10 cm^{-1} was used in the analyses. A cylindrical internal reflectance sampling cell (CIRCLE™, Spectra Tech, Inc., Stamford, CT) with a ZnSe rod crystal in the open boat configuration was fitted into the Digilab instrument.

Humic acid in the form of a sodium salt was obtained from Aldrich Chemical Co. (Milwaukee, WI) and used without further purification. Humic acid solutions with concentrations ranging from 0.5 to 200 g L^{-1} were prepared and stored no longer than 24 h prior to FT-IR analysis. Solutions for ionic strength and pH studies were prepared 0.5 g L^{-1} in humic acid concentration. Ionic strength was adjusted with either $CaCl_2$ or KCl and pH by titration with 2.0 M HCl. Solution pH was adjusted to 7.0 for all samples except those used specifically to determine pH effects. The sample cell chamber was in most instances purged for 1 h with moisture free air prior to spectral data collection. Between each sample analysis the cell was cleaned with acetone followed by water. All spectra were recorded in the absorbance mode from 670 to 4000 cm^{-1} and signal averaged for 1024 scans. Triangular apodization was used to transform the data. Background spectra consisted of the cell filled with water or the appropriate sample matrix. The reported spectra were obtained by referencing the background spectra to the sample spectra. The presented spectra represent those having the highest signal to noise ratio of three replications performed with different solutions. Nujol mull and KBr spectra of Aldrich humic acid were also recorded. A Digilab Qualimatic FT-IR spectrometer with a 7 mm aperature was used to determine these spectra.

RESULTS AND DISCUSSION

Characteristic Absorbance Bands

A spectral scan from 670 to 4000 cm^{-1} indicates that the region of greatest absorbance for humic acid occurs between 1000

and 2000 cm^{-1} (Fig. 2). The spectrum presented depicts a 200 g L^{-1} humic acid solution, thus indicating that work at lower, more realistic natural concentrations approaching the limits of detection, would best be achieved using the 1000 to 2000 cm^{-1} region.

Absorbance peaks at frequencies greater than 3000 cm^{-1} reflect the inability to overcome, through background subtraction, the strong water absorbance centered at 3400 cm^{-1} (Fig. 2). A similar difficulty occurred in previous work with humic acid slurries in which no spectra at frequencies higher than 3100 cm^{-1} were reported (11). The absorbance band located at 2344 cm^{-1} is present in a region usually devoid of any peaks from infrared active functional groups in humic acids and represents CO_2. Carbon dioxide most likely existed in the humic acid solution as a dissolved gas, because increased interferometer chamber purge times failed to remove this absorbance band. Buffering capacity, solution pH, and exposure time to ambient air differed between the water reference and humic acid solutions leading to unequal dissolved CO_2 levels in the two samples.

Major absorbance bands occur at 1050 and 1088 cm^{-1} with increased humic acid concentration increasing the relative intensity of the 1050 cm^{-1} band to a greater extent than the adjacent 1088 cm^{-1} band (Figs. 2,3). In contrast, below humic acid concentrations of 10 g L^{-1}, the 1088 cm^{-1} band becomes dominant of the two (Fig. 4). Infrared activity in the 1000 to 1100 cm^{-1} region has been attributed to C-O stretching of polysaccharides or Si-O stretching of silicate impurities (2). The 1050 cm^{-1} band has been most often considered to represent the presence of polysaccharides (17,18). Silicate contamination is also probable in that Aldrich humic acid has been reported to have an ash content of 31% (16). A primary advantage of CIR is the ability to use humic and fulvic acid extracts prior to freeze-drying. Without freeze-drying, ash removal and purification of humic and fulvic acid is difficult, thus resulting in humic and fulvic acid extracts with relatively high ash levels. Aldrich

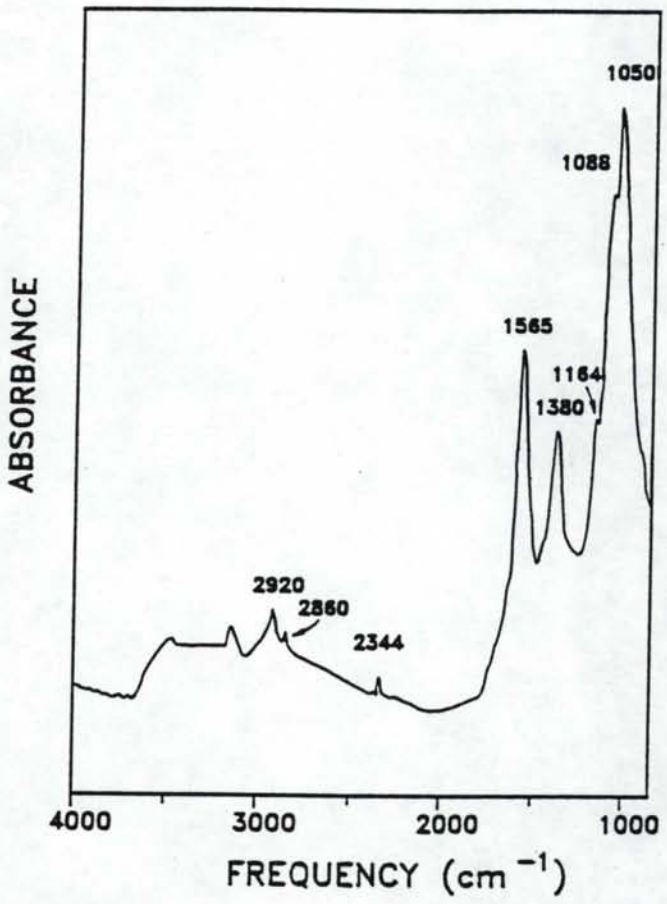

FIGURE 2. FT-IR Spectral Scan of Aldrich Humic Acid (200 g L^{-1}) Using Cylindrical Internal Reflectance.

humic acid ash levels are thus similar to those expected in non-purified preparations from soils. The assignment of absorbance bands to distinct organic functional groups or to inorganic contaminants will thus also be difficult for soil extracts.

An increase in humic acid concentration would decrease the absorbance intensity of functional groups involved in intra- or intermolecular bonding as compared to the absorbance intensity of

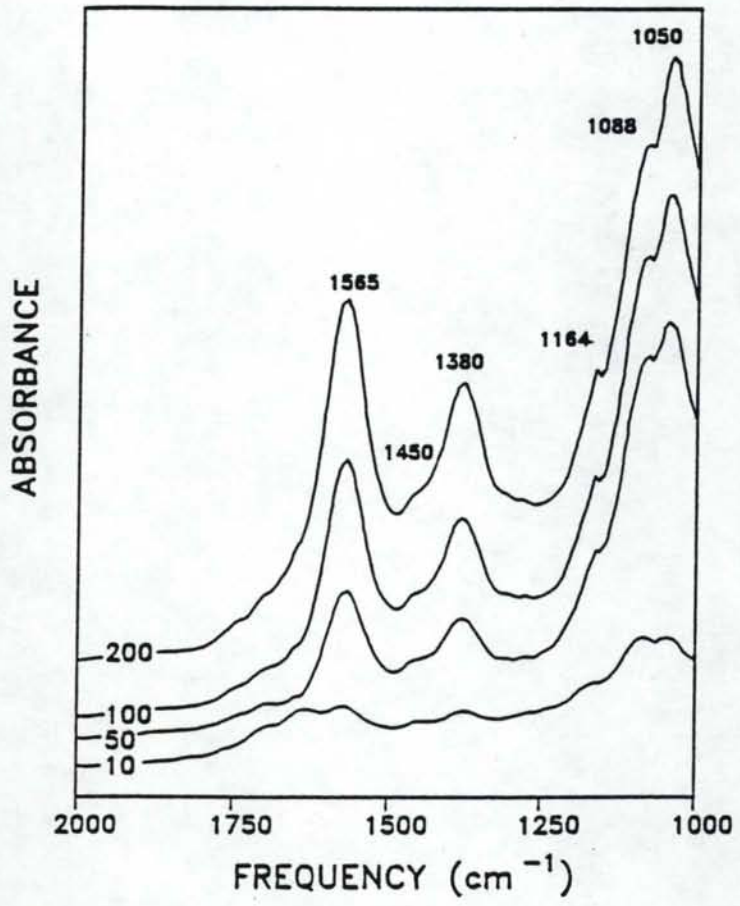

FIGURE 3. FT-IR Spectra of Aldrich Humic Acid in Water at Concentrations from 10 to 200 g L^{-1}.

those groups not involved. Previous work has shown that humic acids behave as rigid, uncharged colloids at concentrations greater than 3.5 to 5.0 g L^{-1}, while at concentrations less than 3.5 g L^{-1} they behave as flexible, linear polyelectrolytes (19). Although a definite functional group assignment cannot be made to either of the two peaks, it is proposed that the interaction of each group may differ when humic acid changes from a colloid to a polyelectrolyte. A functional group participating in intra- or

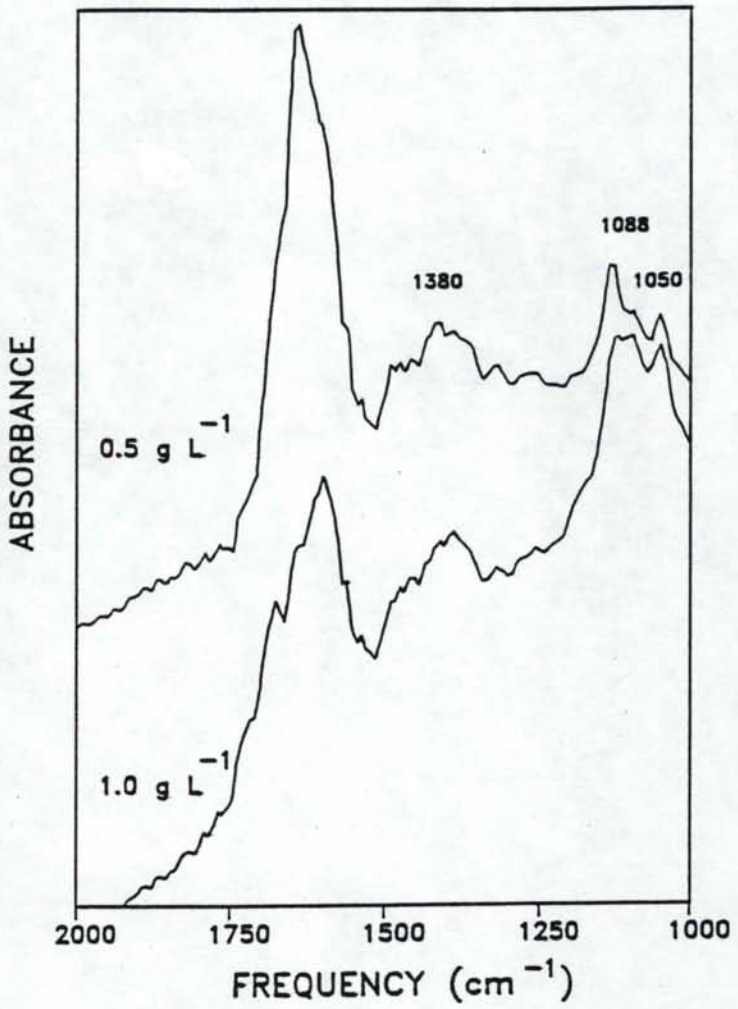

FIGURE 4. FT-IR Spectra of Aldrich Humic Acid in Water at Concentrations of 0.5 and 1.0 g L^{-1}.

intermolecular interaction and colloid formation would increase in intensity with decreased humic acid concentration (1088 cm^{-1} band) relative to a functional group participating to a lesser extent (1050 cm^{-1} band). An alternative explanation exists in that Aldrich humic acid is a heterogeneous mixture of materials varying

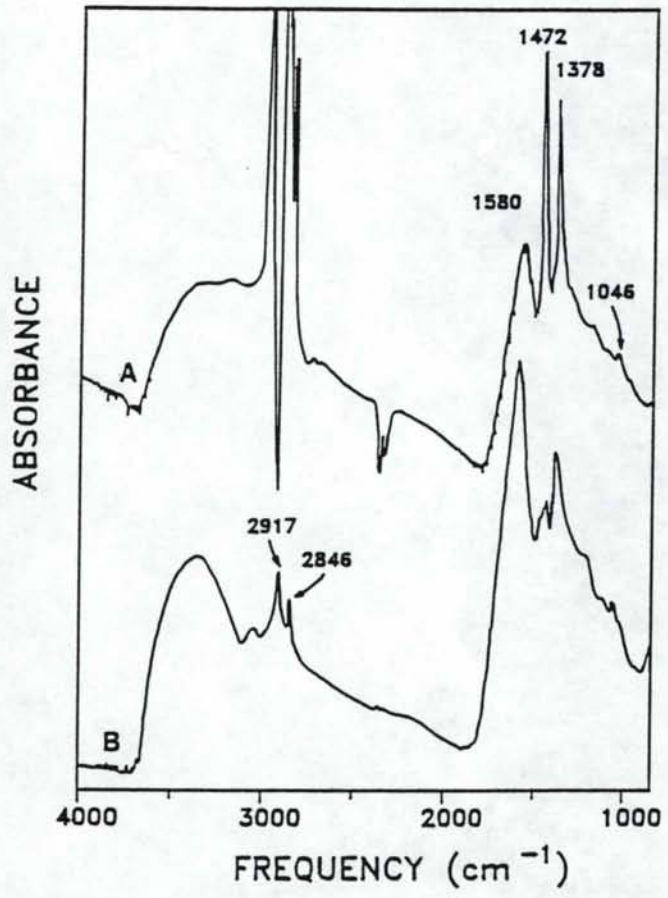

FIGURE 5. Infrared Spectra of Aldrich Humic Acid Determined Using Nujol Mull (A) and KBr (B) Preparations.

in molecular size and functional group chemistries. Precipitation of larger humic acid molecules would occur at lower concentrations than the precipitation of smaller molecules. Selective precipitation of larger molecules would reduce the infrared absorbance of the functional groups of those molecules. The 1050 and 1088 cm^{-1} bands may thus represent different pools of infrared materials precipitating at different humic acid concentrations.

Comparison of CIR spectra to spectra produced using a Nujol mull or KBr pellet of the Aldrich humic acid provide distinct differences in peak absorbance intensity. Peak intensities in the mull and KBr spectra are almost eliminated in the 1000 to 1200 cm^{-1} region as compared to CIR results (Fig. 5). Spectral differences in the 1000 to 1200 cm^{-1} range most likely reflect the effects of hydrogen bonding. Aliphatic C-H groups produce the shoulder peak at 1450 cm^{-1} (1,2,20) (Fig. 3). Increased absorbance at 1472 cm^{-1} in the nonaqueous spectra as compared to CIR spectra indicate increased C-H character of the humic acid even though the same material was used in both instances. This comparison demonstrates that aqueous interactions cause dramatic spectral changes particularly with respect to relative peak heights.

Detection Limits

Precipitation was visually evident at concentrations of 100 and 200 g L^{-1} humic acid, an observation which has been explained based on the formation of a spherocolloid (19). This did not alter the characteristic absorbance bands except to decrease visibility of the 1450 and 1713 cm^{-1} peaks (Fig. 3). Humic acid could be detected at concentrations as low as 0.5 g L^{-1} (Fig. 4). Humic materials exist as linear polyelectrolytes at concentrations below 3.5 g L^{-1} (19), thus indicating that CIR FT-IR is possible on sufficiently low concentrations of humic acid to observe this linear form. This is important when considering practical applications of the CIR technique in that pesticide interactions with humic materials have been shown to depend upon humic material concentration (21,22).

Ionic Strength and pH

Ionic strength was adjusted with both divalent and monovalent cation salts because of the vastly different interaction occurring between each cation and humic acid. Divalent cations such as Ca^{2+} function to electrostatically link negatively charged functional groups on the humic acid molecules causing coagulation (23). This

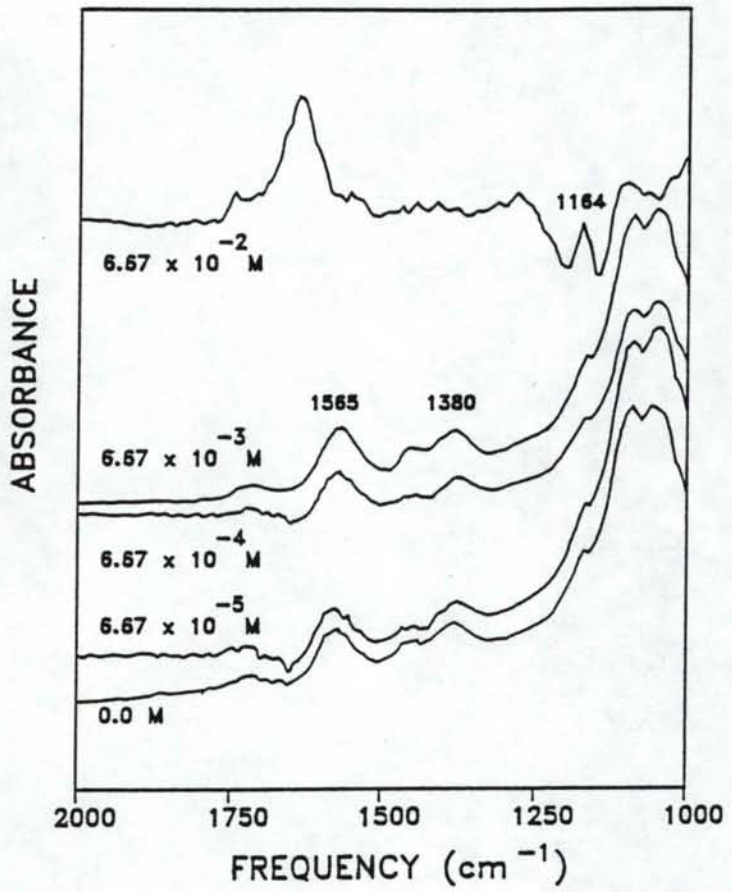

FIGURE 6. FT-IR Spectra of Aldrich Humic Acid in $CaCl_2$ Solution at Levels from 0 to 6.67×10^{-2} M.

was visually observed in the 6.67×10^{-2} M $CaCl_2$ treatment and is evident in the recorded spectrum (Fig. 6). A decrease in band strength or complete elimination is shown for most of the characteristic absorbance bands except for enhancement of the band at 1164 cm^{-1}. Increased signal strength of the 1164 cm^{-1} band may represent an exterior physical location for the responsible functional groups of the colloid as opposed to an internal

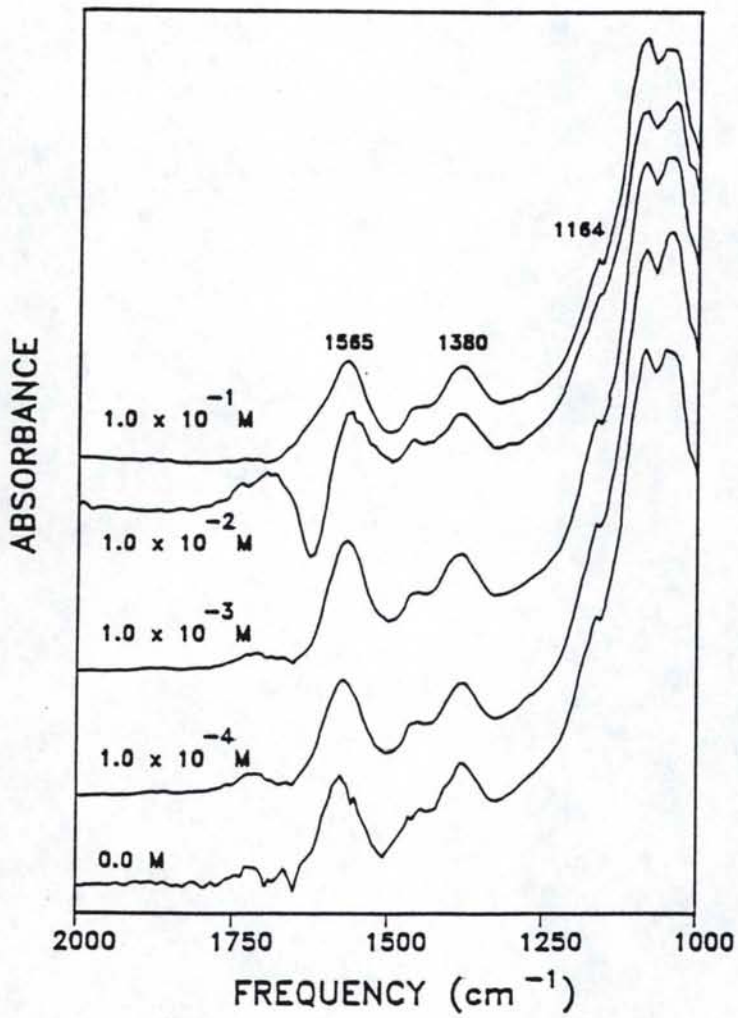

FIGURE 7. FT-IR Spectra of Aldrich Humic Acid in KCl Solution at Levels from 0 to 1.0^{-1} M.

location, or lack of involvement of the responsible functional groups in Ca^{2+} interaction and coagulation.

It has been suggested that upon drying, the polar groups of humic materials orient towards the interior of humic colloids exposing the hydrophobic portions of the material on the exterior

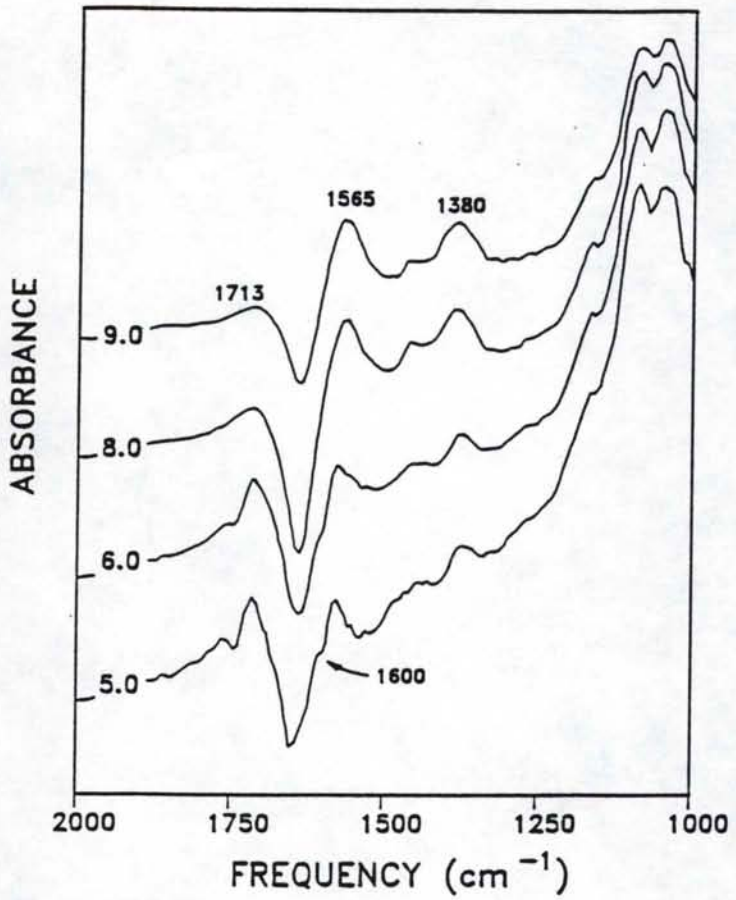

FIGURE 8. FT-IR Spectra of Aldrich Humic Acid Titrated to pH Values Ranging from 5.0 to 9.0.

of the colloid (23). Increased ionic strength may have a similar effect on colloid conformational changes. This behavior has been used to explain increased pyrene binding to estuarine organic matter with increased ionic strength of the solution (24). Conformational changes of humic materials, as dictated by ionic strength, would thus promote similar changes with respect to synthetic organic interactions with soil constituents.

Ionic strength adjustment with KCl would not be expected to show the same alteration of the humic acid spectra as $CaCl_2$ (23). Figure 7 demonstrates that K^+ at a concentration of 1.0×10^{-1} M does not interact with the humic acid in the same manner as does Ca^{2+} and as a result, only small changes in the spectra are observed with all levels of KCl ionic strength adjustment.

Through protonation, titration of the salt form of humic acid to a lower pH would decrease the absorbance bands associated with COO^- groups (1380 and 1565 cm^{-1}) and increase the intensity of the C = O absorbance (1713 cm^{-1}) in those groups (17). A slight decrease in the 1380 and 1565 cm^{-1} peaks is recorded, while a relatively noticeable increase in the 1713 cm^{-1} band is also shown (Fig. 8). A shoulder appears at 1600 cm^{-1} when Aldrich humic acid is titrated to pH values of 5 and 6, indicating behavior similar to that expressed by simple carboxylic acids (1).

The ability to control solution ionic strength and pH is an additional advantage of CIR when considering application of this technique to organic pollutant or trace element interaction studies. For example, the extent of lindane interaction with fulvic acid is highly dependent upon pH and ionic strength (21). DDT binding to humic acid was also shown to be dependent upon pH, ionic strength, and calcium concentration (22). Metal binding to humic materials also responds to pH changes (25,26,27).

Water Absorbance Band

Referencing the sample cell for purposes of background subtraction resulted in variable results with respect to water absorbance at 1640 cm^{-1}. Fluctuations ranging from a negative to a positive absorbance were recorded (Figs. 6-8). No consistent trend was observed with repeated spectra showing a range of possible water absorbance values. It is not known if this is an artifact of the preparation, analysis procedure, or a yet undetermined phenomenon. Recent evidence indicates that water subtraction in the 1640 cm^{-1} region may result in spectral artifacts when using a CIRCLE™ cell with a micro-boat sample

configuration (14). The possibility also exists that two distinct pools of water occur in humic acid solutions. One pool represents free water not associated with the humic material and therefore subtracted in background referencing. A second pool of trapped water interacting through hydrogen bonding to the functional groups of the humic acid might also exist and result in unpredictable absorbance in the 1640 cm^{-1} region.

CONCLUSIONS

Spectra of Aldrich humic acid at concentrations as low as 0.5 g L^{-1} were detected using FT-IR and a CIR sample cell. The ability to use water as a solvent permits the spectra of humic materials to be obtained in solution and at concentration levels sufficient to obtain a linear form. The region of the infrared spectra most suitable for observing characteristic humic acid absorbance bands ranges from 1000 to 2000 cm^{-1}. Comparisons made with nonaqueous Nujol mull and KBr preparations indicate that differences in the spectra result from the presence of water. Changing solvent variables such as pH and ionic strength altered the spectra obtained with respect to functional groups possibly involved in organic pollutant or trace element interaction.

REFERENCES

1. MacCarthy, P. and J.A. Rice. 1985. Spectroscopic methods (other than NMR) for determining functionality in humic substances. p. 527-559. In G.R. Aiken et al. (ed.) Humic substances in soil, sediment, and water. Wiley Interscience, New York.

2. Stevenson, F.J. 1982. Humus chemistry. John Wiley & Sons, New York.

3. Madhun, Y.A., J.L. Young, and V.H. Freed. 1986. Binding of herbicides by water-soluble organic materials from soil. J. Environ. Qual. 15:64-68.

4. Orlov, D.S., O.N. Rozanova, and S. Matyukhina. 1962. Infrared absorption spectra of humic acids. Sov. Soil Sci. 1:15-21.

5. Wagner, G.H. and F.J. Stevenson. 1965. Structural arrangement of functional groups in soil humic acid as revealed by infrared analyses. Soil Sci. Soc. Am. Proc. 29:43-48.

6. Schaumberg, G.D., C.S. LeVesque-Madore, G. Sposito, and L.J. Lund. 1980. Infrared spectroscopic study of the water-soluble fraction of sewage sludge-soil mixtures during incubation. J. Environ. Qual. 9:297-303.

7. Baham, J. and G. Sposito. 1983. Chemistry of water-soluble, metal-complexing ligands extracted from an anaerobically-digested sewage sludge. J. Environ. Qual. 12:96-100.

8. Stevenson, F.J. and K.M. Goh. 1974. Infrared spectra of humic acids: Elimination of interference due to hygroscopic moisture and structural changes accompanying heating with KBr. Soil Sci. 117:34-41.

9. Theng, B.K.G., J.R.H. Wake, and A.M. Posner. 1966. The infrared spectrum of humic acid. Soil Sci. 102:70-72.

10. MacCarthy, P., H.B. Mark, Jr., P.R. Griffiths. 1975. Direct measurement of the infrared spectra of humic substances in water by fourier transform infrared spectroscopy. J. Agric. Food Chem. 23:600-602.

11. MacCarthy, P. and H.B. Mark, Jr. 1975. Infrared studies on humic acid in deuterium oxide: I. Evaluation and potentialities of the technique. Soil Sci. Soc. Amer. Proc. 39:663-668.

12. Bartick, E.G., and R.G. Messerschmidt. 1984. Applications of cylindrical internal reflection for FTIR liquid sampling. Am. Lab. 16:56-62.

13. Bauer, B. and T.A. Floyd. 1987. Monitoring of glucose in biological fluids by fourier-transform infrared spectrometry with a cylindrical internal reflectance cell. Anal. Chim. Acta 197:295-301.

14. Braue, E.H., Jr. and M.G. Pannella. 1987. Consistency in circle cell FT-IR analysis of aqueous solutions. Appl. Spectrosc. 41:1057-1067.

15. Tejedor-Tejedor, M.I. and M.A. Anderson. 1986. "In situ" attenuated total reflection fourier transform infrared studies of the geothite (-FeOOH)-aqueous solution interface. Langmuir 2:203-210.

16. Malcolm, R.L. and P. MacCarthy. 1986. Limitations in the use of commercial humic acid in water and soil research. Environ. Sci. Tech. 20:904-911.

17. Stevenson, F.J. and K.M. Goh. 1971. Infrared spectra of humic acids and related substances. Geochim. Cosmochim. Acta. 35:471-483.

18. Clark, F.E. and K.H. Tan. 1969. Identification of a polysaccharide ester linkage in humic acid. Soil Biol. Biochem. 1:75-81.

19. Ghosh, K. and M. Schnitzer. 1980. Macromolecular structures of humic substances. Soil Sci. 129:266-276.

20. Juo, A.S.R. and S.A. Barber. 1969. Reaction of strontium with humic acid. Soil Sci. 108:89-94.

21. Tramonti, V., R.H. Zienius, and D.S. Gamble. 1986. Solution phase interaction of lindane with fulvic acid: Effect of solution pH and ionic strength. Intern. J. Environ. Anal. Chem. 24:203-212.

22. Carter, C.W. and I.H. Suffet. 1982. Binding of DDT to dissolved humic materials. Environ. Sci. Technol. 16:735-740.

23. Hayes, M.H.B. and F.L. Himes. 1986. Nature and properties of humus-mineral complexes. p. 103-158. In P.M. Huang and M. Schnitzer (ed.) Interactions of soil minerals with natural organics and microbes. Soil Sci. Soc. Amer., Madison, WI.

24. Ostazeski, S.A. and J.C. Means. 1984. The sorption of pyrene on estuarine sediments. J. Am. Chem. Soc. 24:60-61.

25. Ghosh, K. and M. Schnitzer. 1981. Fluorescence excitation spectra and viscosity behavior of a fulvic acid and its copper and iron complexes. Soil Sci. Soc. Am. J. 45:25-29.

26. Perdue, E.M. and C.R. Lytle. 1983. Distribution model for binding of protons and metal ions by humic substances. Environ. Sci. Technol. 17:654-660.

27. Reuter, J.H. and E.M. Perdue. 1977. Importance of heavy metal-organic matter interactions in natural waters. Geochim. Cosmochim. Acta 41:325-334.